

1
2
3
4
5
6
7
8
9
10
11
12
13
14
15
16
17
18
19
20
21
22
23
24
25
26
27
28
29
30
31
32
33
34
35
36
37
38
39
40
41
42
43
44
45
46
47
48
49
50
51
52
53
54
55
56
57
58
59
60

Experimental Study on Charcoal Production from Woody Biomass

Liang Wang*, Øyvind Skreiberg, Sam Van Wesenbeeck, Morten Grønli, Michael

Jerry Antal, Jr.

SINTEF Energy Research

Sem Sælands vei 11, Trondheim, Norway

* Corresponding author: Tel +47 48064531

Email: liang.wang@sintef.no

Submitted to

Special Issue of

In Honor of Michael J. Antal

Experimental Study on Charcoal Production from Woody Biomass

Liang Wang*^a, Øyvind Skreiberg^a, Sam Van Wesenbeeck^{b,c}, Morten Grønli^d, Michael Jerry Antal, Jr.^{b,1}

^a SINTEF Energy Research, Sem Sælands vei 11, Trondheim, Norway

^b Hawaii Natural Energy Institute, School of Ocean and Earth Science and Technology, University of Hawaii at Manoa, Honolulu, Hawaii 96822

^c University Ghent, Biosystems Engineering, Coupure Links 653, 9000 Gent, Belgium

^d Department of Energy and Process Engineering, Norwegian University of Science and Technology, Kolbjørn Hejes vei 1B, Trondheim, Norway

* To whom correspondence should be addressed.

E-mail: liang.wang@sintef.no, Tel.: +47 48064531

¹ Deceased on October 21, 2015.

KEYWORDS: Thermogravimetric analysis, woody biomass, charcoal, fixed carbon, pressure

ABSTRACT

In the present work, effects of process conditions on char and fixed carbon yields from four woody biomasses were studied. Influence of particle size, sample mass and pressure on experimental values of char and fixed carbon yields from spruce stem wood, spruce forest residue, birch stem wood and birch forest residue were examined in three TGAs (two atmospheric and one pressurized) and a flash carbonizer. The obtained experimental fixed carbon yields were then compared with theoretical values calculated using the elemental composition of the studied woody biomasses. It was found that carbonization of small samples of small particles in atmospheric TGAs in an open crucible/pan offered lowest fixed carbon yield. The yields were improved when following standard proximate analysis procedures employing closed crucibles. Further enhancement of the fixed carbon yields were obtained in the atmospheric TGAs using a crucible covered by a lid that restricts release of volatiles. Further, increase of pressure, particle size and sample size gave more significant effects on char and fixed carbon yields. The largest gains were obtained as large particles were carbonized at elevated pressures. The highest char and fixed carbon yields were realized by a flash carbonizer at elevated pressure. Carbonization of spruce wood in the flash carbonizer at 2.2 MPa offered a fixed carbon yield of 28 wt%, which approaches 85% of the theoretical value. SEM analyses revealed significant differences in morphology and microstructure of char particles produced under the different conditions. The spruce wood char particles produced in the flash carbonization reactor passed through a molten stage, showing smooth and intact surface. Melting of cell structure and recondensation/deposition of secondary carbon are more intensive at elevated pressure. The findings presented in this work suggest that secondary reactions, involving interaction of tarry vapors with char and conversion of them to secondary char, play a key role in charcoal

1
2
3 formation. Char and fixed carbon yields from biomass can be considerably enhanced under
4
5
6 process conditions that extend contacts of vapor phases with the char matrix.
7
8
9
10
11
12
13
14
15
16
17
18
19
20
21
22
23
24
25
26
27
28
29
30
31
32
33
34
35
36
37
38
39
40
41
42
43
44
45
46
47
48
49
50
51
52
53
54
55
56
57
58
59
60

1 INTRODUCTION

Extensive use of fossil fuels has caused substantial greenhouse gas emissions and environmental problems. There are urgent needs for alternatives to replace fossil fuels and meet energy demands. In this context, biomass is of significant interest as an affordable, diversified and abundant resource. Bioenergy production can be further developed, with sustainable exploitation of new biomass resources and development or improvement of technologies for efficient conversion of them.

Nowadays, combustion, gasification and pyrolysis are the most common thermochemical conversion routes for recovering energy from biomass. Biomass carbonization is a thermochemical conversion process operating in an inert condition and a moderate temperature range, aiming at converting biomass materials into charcoal, and can be referred to as a low heating rate pyrolysis process ^[1]. The overall biomass charcoal production process includes devolatilization, depolymerization and carbonization of lignocellulosic biomass to generate charcoal as the main output, and tarry vapors and gases ^[2, 3]. When carbonized at moderate temperatures between 400 and 500 °C, a major portion of the initial dry biomass mass is retained as a solid product, the rest become gases and vapors. The carbon content of the solid product can reach 90 wt% or even more, with oxygen content below 6 wt% and hydrogen content near 1 wt% ^[2]. The condensable part of the volatiles can be collected and upgraded into valuable bio-oil and chemicals. The rest can be recirculated or burned to provide heat needed for the carbonization process and improving the process' energy efficiency. In comparison to raw biomass, biomass charcoal has superior properties in terms of combustion applications. Biomass charcoal has significantly lower volatile content and fuel O/C and H/C ratios, compared to the raw biomass ^[1, 4]. This improves the combustion properties, resulting in decreased emissions and energy loss.

1
2
3
4
5
6
7
8
9
10
11
12
13
14
15
16
17
18
19
20
21
22
23
24
25
26
27
28
29
30
31
32
33
34
35
36
37
38
39
40
41
42
43
44
45
46
47
48
49
50
51
52
53
54
55
56
57
58
59
60

Relative to raw biomass, charcoal has much higher fixed carbon content, heating value (per mass unit) and energy density (when compressed) ^[5]. Decomposition reactions during the carbonization process cause biomass to lose its tenacious and fibrous structure. Thereby, charcoal has excellent grindability and is a very homogeneous fuel with respect to particle shape and size after grinding ^[6]. In addition, the amounts of undesired fuel impurities such as nitrogen, sulphur, chlorine and alkalis in the biomass will be considerably reduced during the carbonization process, especially per energy unit ^[7]. It makes biomass charcoal a truly clean fuel, giving reduced impacts on operation and maintenance of combustors. In addition, the biomass charcoal has a great potential to be used as reductant in metallurgical industry. The metallurgical industry consume massive amounts of fossil fuels for using as energy carrier and reductant. They are facing great challenges for mitigating GHG emissions and increasing the sustainability of their production processes ^[8]. Historically, charcoal produced from wood has been intensively used as a fuel and reducing agent in steelmaking industry. In Brazil, the annual production of charcoal is estimated at 9 million tons and 75% of the production is used in the steelmaking sector ^[5]. In addition, there are also great interests in the ferrosilicon industry for using biomass charcoal as alternative to fossil carbon as reductant ^[9]. Consumption of silicon for semiconductors and manufacture of photovoltaic cells are increasing fast. It urges the ferrosilicon industry to increase or implement the use of biomass charcoal for sustainable production and development ^[10]. Compared to the steelmaking industry, the ferrosilicon industry have stricter quality requirements for the charcoal that can be used during the silicon production process. Unfortunately, the carbonization technologies currently used often are technology wise outdated and associated with low efficiency, long production cycle and high emissions ^[2]. Moreover, charcoal produced via current carbonization technologies has rather poor quality and

heterogeneous properties. These properties cause extra difficulties for the metallurgical industries to replace the fossil carbon with biomass charcoal in a high ratio [5, 8].

The charcoal yield is conventionally used as a measure to evaluate efficiency of a biomass carbonization process [11]. The charcoal yield is normally calculated as:

$$y_{char} = \frac{m_{char}}{m_{bio}} \quad (1)$$

where m_{char} is the dry mass of charcoal produced by carbonization of a dry biomass feedstock m_{bio} . Therefore, the charcoal yield y_{char} represents percentage of a dry biomass that remains in the solid product after carbonization under given conditions. However, charcoal contains complex organic chemical compounds and inorganic species and the charcoal yield gives a rather poor quality indication [1]. For the charcoal to be used as a reductant in metallurgical production processes, the fixed carbon content of the charcoal is the most important quality to be taken into account [12]. A new measure for assessing the efficiency of a biomass carbonization process was defined as the fixed carbon yield y_{fc} by Antal et al. [1, 11, 13]. The fixed carbon yield is defined as follows:

$$y_{fc} = \left(\frac{m_{char}}{m_{bio}}\right) \left(\frac{\%fC}{100 - \%feed\ ash}\right) \quad (2)$$

where y_{char} is the charcoal yield, %fC is the fixed carbon content of the charcoal, and %feed ash is the ash content of the dry biomass feedstock [1]. The fixed carbon yield y_{fc} is proposed for assessing the conversion efficiency of ash-free organic matter in the biomass feedstock into fixed carbon. The fixed carbon yield y_{fc} approximates the percentage of pure carbon that can be obtained in the biomass carbonization process. The fixed carbon yield has been widely accepted as an efficient metric for evaluating the efficiency of a biomass carbonization process and the quality of the produced charcoal as well [3, 5, 12, 14].

1
2
3 A number of studies have been carried out focusing on increasing charcoal and fixed carbon
4 yields from carbonization of a wide range of biomass feedstocks [1-3, 5, 11, 15-21]. Several
5 carbonization process parameters were considered and manipulated including peak temperature,
6 heating rate, vapor residence time and pressure. In general, the peak temperature reached during
7 the carbonization process has a decisive effect on the charcoal yield [1, 20]. The charcoal yield
8 decreases as the peak temperature increases. In contrast, increasing peak temperatures leads to
9 increasing fixed carbon content due to the reduction of the volatile matter content in the charcoal
10 [22]. In addition, the surface area and the porosity of charcoal normally increase with increasing
11 process temperature [23]. Heating rate has a crucial effect on products distribution in a pyrolysis
12 process. Low heating rates favor high charcoal yields. It has been revealed that charcoal contains
13 primary and secondary charcoal. The latter one is formed as a result of secondary reactions of
14 volatile compounds, tars, inside the microstructure and in the immediate vicinity of charcoal
15 particle surfaces [1, 3]. Longer vapor residence time favors secondary reactions of these volatile
16 species and formation of secondary charcoal, resulting in enhancement of charcoal and fixed
17 carbon yields [11]. Compared to other influencing parameters, pressure is one less studied
18 parameter that influences the carbonization process and product yields. Antal and coworkers
19 have carried out continuous work to study the effect pressure on the biomass carbonization
20 process, pursuing maximum charcoal and fixed carbon yields from various biomass feedstocks.
21 Antal et al. investigated formation of charcoal from cellulose and biomass in a sealed (constant
22 volume) reactor under pressures between 3 and 14 MPa [1, 11-13, 16, 17, 24-27]. For cellulose, a fixed
23 carbon yield of 40% was realized and this value is quite close to the theoretical maximum yield
24 of 46% for this substance [18]. Enhancement of char yields of biomass feedstocks were also
25 obtained by employing the sealed pressurized reactor. Later, Antal and coworkers designed and
26
27
28
29
30
31
32
33
34
35
36
37
38
39
40
41
42
43
44
45
46
47
48
49
50
51
52
53
54
55
56
57
58
59
60

1
2
3 built a pressurized laboratory scale flash carbonization reactor. Diverse biomass species were
4 carbonized in this reactor under different pressures in the range of 1 to 3 MPa [11, 13, 16, 17, 28].
5
6 Significant enhancement of charcoal yield and fixed carbon yield were realized from
7 carbonization of these biomass species. The increase of charcoal and fixed carbon yield is mainly
8 attributed to enhancement of secondary reactions associated with cracking, repolymerization and
9 recondensation of tarry vapors [11, 13]. In addition, elevated pressure is favored to reduce both
10 carbonization time and onset temperature [13]. In recent studies, Antal and coworkers studied
11 carbonization of Avicel cellulose in a sealed tubing bomb at elevated pressure. It was found that
12 carbonization of Avicel cellulose took place at much lower temperatures than customary at
13 atmospheric pressure [18, 29]. This pioneer work for the first time reported an experimental fixed
14 carbon yield that exceeds the theoretical value derived from thermodynamic calculations [18]. The
15 effect of pressure on biomass carbonization behaviors and product yields has also been studied
16 by other researchers. It was found that fixed carbon yields are affected by both pressure and peak
17 temperature [5, 19-21]. In addition to process parameters, intrinsic properties of biomass feedstocks,
18 including moisture content, ash content and composition, particle size, and lignin content, have
19 also considerable effects on biomass carbonization product yields and distributions [1, 3, 5, 30, 31].
20 Our previous work reported that particle size strongly influences charcoal and fixed carbon yield
21 at pressures in the range from 0.1 to 2.7 MPa [10]. In larger biomass particles, vapor residence
22 time is longer, prolonging the contact time between vapors and the solid matrix. This causes
23 enhancement of the secondary reactions and increase of fixed carbon yield.
24
25
26
27
28
29
30
31
32
33
34
35
36
37
38
39
40
41
42
43
44
45
46
47
48
49
50

51 Improvement of fuel flexibility is a key issue that can boost development and commercialization
52 of biocarbon production. Conventional biocarbon production has been restricted to woody
53 biomass [5]. However, more less expensive and large amount available biomass materials should
54
55
56
57
58
59
60

1
2
3 be searched for and tested, considering increasing scarcity of virgin wood and its high production
4 costs, along with increasing labor costs. Additionally, a biocarbon production process is flexible
5
6 with respect to particle size and moisture content of feedstocks. This makes it possible to adopt a
7
8 biocarbon production process to a variety of low-grade and non-traditional biomass materials ^[8].
9
10 Detailed investigations are required to derive indicative optimum process parameters based on
11
12 the physical properties and chemical compositions of different biomass types. Full-scale
13
14 biocarbon production tests for various biomass materials are needed to obtain operational data
15
16 and an optimum operating spectrum. Moreover, combined with a densification (i.e. pelletization,
17
18 briquetting) process, a biocarbon production process provides a volume and energy dense fuel
19
20 that can be handled, transported and stored with low logistic expenses ^[4]. It might help to
21
22 improve the economic characteristics of low-grade fuels (i.e. forest residues) and offer
23
24 opportunities to achieve profitable biomass-to-energy value chains.
25
26
27
28
29
30
31

32
33 The specific scope of the present study is to study the effect of carbonization process conditions
34
35 (pressure, vapor residence time and particle size) on char and fixed carbon yield of woody
36
37 biomasses including spruce stem wood, spruce forest residue, birch stem wood and birch forest
38
39 residue. To the best of our knowledge, carbonization of forest residues under various pressures
40
41 and gas residence times has not been reported. The carbonization experiments were conducted in
42
43 atmospheric and pressurized thermogravimetric analyzers (TGAs) under well controlled
44
45 conditions. The results reveal the importance of carbonization conditions on charcoal formation
46
47 for the studied woody fuels and suggest possibilities for efficiently producing charcoal from also
48
49 low-grade forest residue.
50
51
52
53
54
55
56
57
58
59
60

2 EXPERIMENTAL SECTION

1
2
3
4
5
6 Spruce stem wood, spruce forest residue, birch stem wood and birch forest residue were studied
7
8 in the present work. The spruce and birch trees were harvested from a Norway spruce forest
9
10 (Latitude 59°38'N, Longitude 09°09'E) and a birch forest (Latitude 59°55'N, Longitude 10°89'E)
11
12 in South Norway. The harvested trees were separated into three fractions: stem wood, forest
13
14 residue (containing top and branches) and stump wood and then transported out of the forest. The
15
16 three fractions were stored for further analysis and experiments. In such a way, only the top and
17
18 branches are used as representative for forest residue, and without mixing with pieces previously
19
20 falling down on the ground or contaminations like stone and sand. The spruce and birch stem
21
22 wood and their forest residues were further shredded into small pieces. The shredded stem wood
23
24 and forest residues were further shredded into small pieces. The shredded stem wood
25
26 and forest residue were dried at 105 °C for 24 hours and stored in plastic containers before using.
27
28
29

30
31 The pre-dried spruce and birch stem wood and their forest residues were ground in a cutting mill
32
33 (IKA MF 10) mounted with a 1 mm sieve. The four ground wood samples were subjected to
34
35 proximate analysis according to American Society for Testing and Materials (ASTM) E871 and
36
37 E872. The ash content of the four samples was determined through following the procedures
38
39 described in standard ASTM D1102. Elemental (C/H/N/S) compositions of the four dried wood
40
41 samples were analyzed by employing an Eurovector EA 3000 CHNS-O elemental analyzer. The
42
43 inorganic element compositions of the four samples were analyzed by inductively coupled
44
45 plasma optical emission spectrometry (ICP-OES, Thermo Scientific iCAP 6300 Duo View
46
47 Spectrometer) according to standard CEN/TS 15290:2006.
48
49
50

51
52
53 Two atmospheric pressure thermogravimetric analyzers (TGAs): TA Q5000 (TA Instrument) and
54
55 Mettler Toledo TGA 851^e (MT TGA) were employed in the present work. Prior to one
56
57 experiment, 10 mg ground sample was loaded into an alumina crucible or a platinum pan. Each
58
59
60

1
2
3 experiment started with 30 minutes purging at room temperature, which was followed by drying
4
5 at 105 °C for 30 minutes. The sample was then heated up from 105 °C to 950 °C at a heating rate
6
7 of 10 °C/min. The same temperature program was used in our previous work^[10, 12]. Two types of
8
9 atmospheric TGA experiments were performed: using an open crucible with sample loaded (i.e.,
10
11 no lid) and a loaded crucible covered by a lid with a small pinhole. The latter one is identified as
12
13 closed crucible experiments. For some experiments performed in the MT TGA, a large crucible
14
15 (900 μ l) was used and around 100 mg sample was loaded for charcoal production. In addition,
16
17 the large crucible was also covered by a lid with a small pinhole to perform closed crucible
18
19 experiments. Table 1 summarizes the geometry and depth of the crucible and the pan used with
20
21 each TGA. The dimension and depth of one crucible might affect the egress of volatiles from the
22
23 pyrolyzing solid and the contact time with the char matrix, and char and fixed carbon yields
24
25 consequently. The different char and fixed carbon yields from one sample by using different
26
27 crucibles are reported and discussed in the following sections. For all atmospheric experiments,
28
29 pure nitrogen was used as purge gas with a flow rate of 100 mL (NTP conditions)/min. The char
30
31 yield y_{char} was calculated dividing the sample mass as measured at 950 °C by the mass measured
32
33 at the end of the drying stage at 105 °C. For each sample, at least three runs under the same
34
35 experimental conditions were performed and average values of these runs are presented in the
36
37 following section. The experimental data indicate a high repeatability of experiments performed
38
39 in the three TGAs under atmospheric pressure. Some variation of char yields was observed for
40
41 experiments conducted with forest residues under pressures. The maximum deviation of the char
42
43 yield was $\pm 1.2\%$ for three carbonization experiments repeated for birch forest residues at 22 bar
44
45 pressure.
46
47
48
49
50
51
52
53
54
55
56
57
58
59
60

1
2
3 A pressurized thermogravimetric analyzer (Linseis STA HP-TGA) was also employed to study
4 charcoal production from the four woody biomasses at various pressures. The pressurized
5 thermogravimetric analyzer (PTGA) consists of a lower horizontal pressure vessel and an upper
6 vertical pressure vessel. The balance beam and weighing unit are located in the lower vessel. The
7 balance beam connects to a vertical ceramic rod with a sample holder on top of it. The ceramic
8 rod is in a ceramic furnace that is surrounded by a graphitic heating element and thermal
9 insulation materials. The furnace, heating element and thermal insulation materials are all located
10 in the upper pressurized vessel. The upper vessel and part of the lower vessel were water cooled,
11 in order to prevent temperature overshoot. The lower and upper vessels are connected by a
12 central flange kit. The PTGA is designed for a maximum operation temperature of 1100 °C and
13 pressure of 55 bar. Prior to each experiment, the upper pressure vessel was moved up vertically
14 to an upper end position. It enables placement of an alumina crucible with sample loaded on the
15 sample holder. In the present work, 10 mg sample was loaded in an alumina crucible for a PTGA
16 experiment. Then the upper vessel was moved down and contacted with the lower vessel, then
17 they were connected by fastening the central flange kit. After sample loading and closing the
18 PTGA system, the vessels were vacuumed to remove air. Then nitrogen (99.999% pure) was
19 introduced into the lower vessel to generate the desired pressure in the PTGA. As the set
20 pressure was reached, nitrogen (99.999% pure) gas was introduced through a gas inlet located on
21 top of the furnace, for generation of an inert atmosphere. The nitrogen gas flows downward and
22 surrounds the sample holder. The nitrogen gas flows further downward and mixes with the
23 nitrogen purge gas in the lower part of the furnace, and then leaves the lower pressure vessel.
24 After stabilization of the balance and pressure, the temperature program was started, which is the
25 same as the one used for the atmospheric TGA experiments. The volume and size of the PTGA
26
27
28
29
30
31
32
33
34
35
36
37
38
39
40
41
42
43
44
45
46
47
48
49
50
51
52
53
54
55
56
57
58
59
60

1
2
3 crucible are listed in Table 1. Two types of pressurized TGA experiments were performed for
4
5 studying effects of pressure and gas residence time on charcoal formation from the studied
6
7 woody biomasses. The first series of experiments were carried out with a constant flow rate of
8
9 pure nitrogen at elevated pressure. For comparing those experiments performed with atmospheric
10
11 TGAs, 100 mL min⁻¹ nitrogen gas flow was introduced for running the first series of
12
13 experiments. The second series of experiments were performed at a constant true volumetric
14
15 flow rate at different pressures. In other words, the superficial gas velocity, hence residence time,
16
17 was maintained for the second series of experiments. Therefore, flows of 800 and 2200 mL min⁻¹
18
19 nitrogen were actually used for the 0.8 and 2.2 MPa pressure experiments. To study the effect of
20
21 particle size on charcoal and fixed carbon yields, 10 grams of each ground sample were sieved.
22
23 Char yields from particles in the size range 63 < *d* < 100 and 300 < *d* < 600 μm were measured
24
25 using the PTGA at elevated pressures. Both open and closed crucible experiments were
26
27 performed for sieved samples.
28
29
30
31
32
33

34
35 The spruce wood was also carbonized in the flash carbonization reactor at University of Hawaii.
36
37 Details about the reactor and normal operational procedures were described in our previous work
38
39 [10, 12]. In the present work, a total of 0.7 kg of spruce wood was placed in a canister that is loaded
40
41 into a pressure vessel. The pressure vessel was pressurized with air to a set value. In the present
42
43 work, the spruce wood was carbonized at pressures of 0.8 and 2.2 MPa, respectively. After
44
45 pressurizing the reactor to the desired pressure, the loaded spruce wood was ignited by an
46
47 electrical heating coil at the bottom of the pressure vessel. The ignitor was turned off after 6
48
49 minutes ignition time. Following the ignition, compressed air was delivered to the top of the
50
51 reactor and flowed downward through the feedstock bed. At the same time, ignition caused flash
52
53 fire of feedstock and the flame front moved upward and against the flow of air, triggering the
54
55
56
57
58
59
60

1
2
3 conversion of feedstock into charcoal. The pressure in the reactor was continuously monitored
4 and maintained at a set value by a valve located downstream of the reactor. After sufficient air
5 was delivered to carbonize the wood, the airflow was halted and the reactor cooled down. The
6 charcoal produced from one experiment was collected and equilibrated under a fume hood for 2
7 days. Then the charcoal samples were subjected to proximate analysis according to ASTM D
8 1762-84.
9
10
11
12
13
14
15
16
17

18 A scanning electron microscope (SEM, Hitachi S-3400N) was employed for exploring
19 microstructure and surface morphology of the charcoal produced from the TGAs and the FC
20 reactor. The FC charcoal was first ground to particles with size less than 1 mm. Samples were
21 mounted on carbon tape without further treatment and then further scanned by the SEM.
22
23
24
25
26
27
28

29 **3 RESULTS AND DISCUSSION**

30 3.1 Fuel characterization

31
32 Table 2 summarizes proximate analysis results, heating values and fixed carbon yields of spruce
33 wood, spruce forest residue, birch wood and birch forest residue. It is clear to see that spruce and
34 birch forest residue have significantly higher ash content than those of the stem woods. It has
35 been reported that ash contents of samples from different parts of trees are considerably
36 different. The twigs, shoots and needles often have 10 to 20 times higher ash content than stem
37 wood^[32, 33]. The forest residues studied in the present work contain mainly branches and tops,
38 which explains the high ash content of them as determined by the proximate analysis. Table 2
39 shows that, even with evidently high ash content, the calculated fixed carbon content of spruce
40 and birch forest residues are still higher than their counterpart stem wood. The proximate
41 analysis can be considered as a kind of carbonization process. It enables us to calculate the fixed
42 carbon yield y_{fc} realized in the proximate analysis. For the spruce and birch wood, the y_{fc} values
43
44
45
46
47
48
49
50
51
52
53
54
55
56
57
58
59
60

1
2
3 are 17.0 wt% and 14.9 wt%, respectively. These values are slightly higher than those obtained
4
5 from oak wood and sweet gum reported in our previous work ^[10]. On the other hand, it is
6
7 interesting to see that the fixed carbon yield of both spruce and birch forest residue are
8
9 considerably higher, respectively 21.7 wt% and 18.7 wt%. From this point of view, forest
10
11 residues studied in the present work are more promising feedstocks than stem wood for charcoal
12
13 production.
14
15
16
17

18
19 Table 3 shows ultimate analysis results and theoretical fixed carbon yields of the studied
20
21 feedstocks. The carbon contents of spruce and birch forest residue are slightly higher than in the
22
23 studied stem woods. The ultimate analysis results were used to calculate yields of pyrolysis
24
25 products by using the STANJAN software when chemical equilibrium is achieved at 400 °C and
26
27 0.1 MPa ^[34]. The calculated theoretical fixed carbon yield y_{fc} of spruce and birch wood are quite
28
29 close, respectively 33.6 wt% and 33.7 wt%, as they have similar elemental composition as shown
30
31 in Table 3. For spruce and birch forest residue, the theoretical fixed carbon yield y_{fc} are 37.5
32
33 wt% and 35.3 wt%, respectively. From a theoretical standpoint, the forest residues studied in the
34
35 present work are better than stem wood for producing charcoal containing more fixed carbon.
36
37 One should note that the theoretical fixed carbon yield values are almost twice those realized by
38
39 proximate analysis as shown in Table 2. The proximate analysis procedures are similar and
40
41 relevant to a conventional practical charcoal production process. Direct comparison of theoretical
42
43 fixed carbon yields and possible yields realized by practice implies supersizing the poor
44
45 efficiency of conventional charcoal production processes. Development and optimization of
46
47 carbonization processes are needed for improving and/or maximizing fixed carbon yield and
48
49 carbon conversion efficiency as well.
50
51
52
53
54
55
56

57 3.2 Effect of vapor residence time on char and fixed carbon yield
58
59
60

1
2
3 A round-robin study of char and fixed carbon yields from ground samples were carried out in the
4 present work by employing three thermogravimetric analyzers (TGAs). Figures 1 and 2 display
5 char yields from the four woody biomasses obtained in each TGA. For all four woody
6 biomasses, the lowest char yields were obtained by employing the TA Q5000. The pressurized
7 TGA realizes significantly higher char yields than the other two. Compared to the other two
8 TGAs, a shallow pan with low rim was used for running pyrolysis experiments with the TA
9 Q5000. In addition, the purge gas flows in as a crossflow in the upper vicinity of the sample and
10 carry away the volatiles produced during one experiment. Therefore, the residence time of
11 volatiles including tarry vapors inside and outside particles is short. It hinders secondary
12 reactions and char yield consequently. In contrast, both the MT TGA and PTGA employ deep
13 and narrow crucibles that isolate samples from the purge gas flow, prolonging contacts of vapor
14 phases with solid char and enhancing secondary reactions. It explains higher char yields realized
15 by employing the MT TGA and partly in the PTGA.
16
17
18
19
20
21
22
23
24
25
26
27
28
29
30
31
32
33
34

35 Figures 3 and 4 display char yields of the four woody biomasses measured by the MT TGA at
36 950 °C with two different sample masses and with open and closed crucible. As shown in
37 Figures 3 and 4, the char yields of ground samples clearly depend on sample mass. 10 mg spruce
38 and birch wood samples in the open crucible offered char yields of 18.9 wt% and 16.0 wt%
39 respectively, that increased to 23.3 wt% and 19.9 wt% with 100 mg sample, respectively. Similar
40 as for the wood samples, in an open crucible, the char yield of 10 mg spruce and birch forest
41 residue increased from 22.8 wt% and 21.2 wt% to 27.7 wt% and 25.4 wt%, respectively. For
42 both 10 and 100 mg samples, the closed crucible experiments show significant improvement of
43 fixed carbon yields. These findings agree well with what have been reported in our previous
44 work, where considerable improvement of char yields were realized as wood samples with larger
45
46
47
48
49
50
51
52
53
54
55
56
57
58
59
60

1
2
3 initial masses were employed ^[10, 12]. As a certain amount of ground sample particles is loaded
4 into a crucible, a sample layer is formed and the thickness of the layer is in relation to sample
5 mass, sample particle size and dimension of the crucible. In the present work, the thickness of
6 the 100 mg sample bed is evidently larger than that of the 10 mg case. A longer runaway time of
7 pyrolysis vapors in the thicker 100 mg sample bed can be expected. Hence, conversion of
8 pyrolysis vapors into secondary carbon is more intensive, leading to increase of char and fixed
9 carbon yield. The char samples remaining in the TGA with a 100 mg initial raw sample enables
10 us to run proximate analysis with the TGA according to procedures described in ASTM E 1131-
11 08. With the proximate analysis results, values of the fixed carbon yields for a sample mass of
12 100 mg when using open and closed crucibles in the MT TGA are estimated, and are listed in
13 Table 4. The \pm values associated with represent the sample standard deviation of three (for
14 spruce and birch wood) to five (spruce and birch forest residue) identical runs with the MT TGA.
15 In all cases, using a closed crucible resulted in increased fixed carbon yields by about 10-15%.
16 One should note that the fixed carbon yields realized with the 100 mg samples are significantly
17 higher than those obtained by the proximate analysis procedure (Table 2). However, even for the
18 experiments with closed crucible, the realized fixed carbon yields are still evidently lower than
19 the theoretical fixed carbon yields (Table 3).

3.3 Effect of sample size on char and fixed carbon yield

20 To study the effect of particle size on char yield at elevated pressures, 10 g of each ground
21 sample was sieved and char yields were measured for the sieved samples with size in the range
22 of $63 < d < 100$ and $300 < d < 600 \mu\text{m}$ using the PTGA. Figures 7 and 8 display the influence of
23 particle size and pressure on char yields for the four woody biomasses. For comparison purpose,
24 the char yields from samples with size $d < 1000 \mu\text{m}$ are included and shown in Figures 7 and 8.
25 Clearly, for all samples, the particle size has a considerable effect on the char yield at elevated
26
27
28
29
30
31
32
33
34
35
36
37
38
39
40
41
42
43
44
45
46
47
48
49
50
51
52
53
54
55
56
57
58
59
60

1
2
3 pressures. The steady increase in yield with increasing particle size has been observed in our
4
5 previous work, as sweet gum, oak wood and corncob were pyrolyzed in an atmospheric TGA ^{[10,}
6
7 ^{12]}. Figures 7 and 8 show that the same trends were obtained in the present work, as samples with
8
9 different particle sizes were pyrolyzed at atmospheric pressures. In good agreement with findings
10
11 of the present work, effects of particle size on products yields from pyrolysis of biomass have
12
13 been reported earlier by employing thermogravimetric analyzers. Hayat et al. reported that
14
15 changing the particle size of studied wood samples has a consistent effect on char yields ^[35].
16
17 Higher char yields were obtained from larger particles. It is attributed to greater intraparticle
18
19 mass transfer resistance and increased residence time in the large particles, which increased
20
21 opportunities for heterogeneous secondary reactions and formation of secondary char as well ^[35].
22
23 In another study, effects of particle size on char yield, thermal reactivity and decomposition rate
24
25 of hazelnut shell was studied by conducting pyrolysis experiments with a thermogravimetric
26
27 analyzer ^[36]. Hazelnut shell particles with size in the range of 0.15 to 1.4 mm were pyrolyzed in
28
29 the TGA with a linear heating rate of 20 K/min from ambient temperature to 1173 K. It was
30
31 reported that the char yields were lower for the smaller particles. Compared to the large particles,
32
33 the smaller particles have overall significantly greater outer surface area but less diffusion
34
35 resistance for the pyrolysis vapors ^[36]. This does not favor secondary char forming reactions.
36
37 Influence of particle size on wheat straw pyrolysis in a thermogravimetric analyzer was
38
39 examined for a particle size in the range between 150 and 1350 μm ^[37]. For particles larger than
40
41 250 μm , the char yields increased with the increasing particle size in the sample. During
42
43 pyrolysis, the concentration of tarry vapors in the bigger char particles are higher than in the
44
45 smaller ones. It implies more intensive secondary reactions of the tarry vapors and recombination
46
47 of them on internal surfaces of char particles ^[38]. Moreover, the intraparticle mass transfer
48
49
50
51
52
53
54
55
56
57
58
59
60

1
2
3 resistance increases with increasing particle size, causing confinement of tarry vapors in the char
4 matrix. Consequently, formation of secondary char is more intensive in large particles, resulting
5
6 in increase of char yield. Figures 7 and 8 display that the char yield increased with increasing
7
8 particle size as the samples were pyrolyzed at elevated pressures. The highest char yields were
9
10 obtained from samples with the largest particles at a pressure of 2.2 MPa. The similar positive
11
12 effect of particle size on char yields were also reported in several studies as various biomass
13
14 materials were pyrolyzed in a bench scale cylindrical reactor and a fluidized bed reactor [22, 39, 40].
15
16
17 In recent work, pyrolysis volatiles produced during slow pyrolysis of beech wood particles were
18
19 characterized by means of laser-induced fluorescence [41, 42]. The results showed, compared to
20
21 small particles, that more intensive secondary cracking reactions of primary tar species occurred
22
23 in large particles. These secondary cracking reactions are exothermic and heat from these
24
25 reactions promote formation of polyaromatic hydrocarbons and secondary char as well. Figures
26
27 5-8 show that char yields of spruce and birch forest residues are higher than those obtained from
28
29 their counterpart stem wood. This is partially attributed to high contents of mineral matter in the
30
31 forest residues. It is well known that metal ions as K, P, Ca, Fe and Cu in biomass material can
32
33 greatly promote char formation [26, 30, 43].
34
35
36
37
38
39
40
41

42 3.4 Effect of pressure on char and fixed carbon yield

43
44 Figures 5 and 6 display impacts of pressure and use of open and closed crucible on char yields
45
46 from spruce and birch wood and their respective forest residues. Significant improvements of
47
48 char yields were realized as one sample was pyrolyzed under elevated pressure in an open
49
50 crucible. To the best of our knowledge, this is the first time that char yields of forest residues are
51
52 studied via employing a pressurized thermogravimetric analyzer. For spruce and birch wood
53
54 samples, as they were pyrolyzed at a pressure of 2.2 MPa in open crucibles, the char yields
55
56
57
58
59
60

1
2
3 increased by about 3-6%. The effects of pressure on char yields are more evident for the spruce
4 and birch forest residues. As shown in Figure 5, the 10 mg spruce forest residue char yield was
5
6 24.3% and further increased to 30.9% and 32.5% for the 0.8 MPa and 2.2 MPa experiments. The
7
8 behaviors of the birch forest residue was similar to that of spruce forest residue: the char yield
9
10 increased from 22.9% to 25.9% and 28.5% for 0.8 and 2.2 MPa experiments. Effects of pressure
11
12 on distribution of biomass pyrolysis reactions and char yields have been studied earlier. Antal
13
14 and coworkers carried out a number of studies with different experimental setups to evaluate
15
16 impact of pressure on pyrolysis reactions and char yield of cellulose and various biomass
17
18 materials ^[11, 16, 24, 25, 27]. It is generally known that gains in char yields can be realized by
19
20 increasing the process pressure. Under pressure, the pyrolysis vapors have a smaller specific
21
22 volume, resulting in longer intraparticle residence time for them. As the vapors escape from the
23
24 biomass particles, decomposition rates of these highly reactive vapors are enhanced, promoting
25
26 formation of secondary carbon and improving char and fixed carbon yields ^[27]. In addition,
27
28 partial pressure (concentration) of the pyrolysis vapors are higher at elevated pressure. It favors
29
30 secondary reactions of these vapors from a thermochemical equilibrium point of view. Moreover,
31
32 under pressurized condition, both carbonaceous materials and inorganic elements dispersed in a
33
34 pyrolyzing char particle play a more active role as catalysts ^[44]. Catalytic role of the pyrolyzing
35
36 char and inorganic elements leads to enhanced formation of secondary carbon from the pyrolysis
37
38 vapors ^[44, 45]. For biomass materials, the char is formed from primary and secondary reactions.
39
40 The latter one is related to cracking, oxidization, re-polymerization and condensation of tarry
41
42 vapors produced from primary pyrolysis ^[30]. Presence of the ash forming matters in the nascent
43
44 char particle promotes the decomposition of the tarry vapors and formation of secondary chars
45
46 and gases. The catalytic effects of ash on pyrolysis behaviors and char yield of various biomasses
47
48
49
50
51
52
53
54
55
56
57
58
59
60

1
2
3 have been studied previously ^[30, 44, 45, 49]. In general, higher charcoal yields were realized from
4 biomass materials with high ash content or impregnated by mineral matters, including wood,
5 agricultural residues (i.e., wheat and rice straw) and food processing residues (i.e., coconut shell)
6 ^[30, 44, 45, 49]. On the other hand, reducing ash in the biomass materials by deashing or washing
7 caused considerable decrease of char and gas yields and increase of tar yields ^[30, 45, 49]. In
8 addition to absolute content of the ash in one biomass, chemical compositions of ash may also
9 have significant impact on conversion of tarry vapors into permanent gases and refractory coke.
10 For biomass materials, most of the ash forming matters present are in the form of cations (i.e., K,
11 Na and Ca) in the organic matrix or in the form of precipitates as salts in the substrate of the
12 organic structure ^[32, 33, 44, 49]. Cations including potassium and sodium showed stronger effects on
13 cracking of tarry vapors and formation of char. However, other elements like silicon has little
14 effect on pyrolysis chemistry and char formation ^[33, 49-51].
15
16
17
18
19
20
21
22
23
24
25
26
27
28
29
30
31

32 Increase of pressure positively affects secondary reactions from different aspects and contributes
33 to improved char and fixed carbon yields. It is worth noting that the experiments corresponding
34 to the results shown in Figures 5 and 6 were performed with a constant flow rate of 100 mL min⁻¹
35 ¹. The true volumetric gas flow rate decreases at elevated pressures. In other words, the
36 superficial gas flow velocity will decrease in the PTGA as the pressure increases, which reduces
37 the diffusivity of the pyrolysis vapors. It prolongs the residence time of pyrolysis vapors inside
38 and in the vicinity of the pyrolyzing particles due to increase of pressure. Therefore,
39 enhancement of char yields of all samples shown in Figures 5 and 6 are attributed to elevated
40 pressure and extension of vapor residence time. Closed crucible experiments were also carried
41 out at elevated pressures and results are shown in Figures 5 and 6. In virtually all cases, the char
42 yields increased due to closure of the crucible. Covering of one crucible with a lid significantly
43
44
45
46
47
48
49
50
51
52
53
54
55
56
57
58
59
60

1
2
3 isolates the sample and pyrolysis products from the purge gas. It limits effects of gas flow on
4 diffusivity of pyrolysis vapors produced during one experiment. In addition, as described above,
5 using a lid restricts escape of pyrolysis vapors out of the crucible and favors attainment of higher
6 char yields. Effects of pressure on the pyrolysis of coal have been studied. Chen et al. reported
7 that yields of char from low coals in a pressurized TGA slightly increased at elevated pressures
8 [46]. The effects of pressure on sample pyrolysis behaviors and products yields were more evident
9 as the temperature was above a critical temperature for one studied coal sample [46]. However, for
10 biomass materials, studies conducted in a pressurized TGA to investigate influences of pyrolysis
11 conditions is rarely available. Manya et al. conducted experiments in a pressurized TGA to
12 investigate effect of pressure and peak temperature on char yield during pyrolysis of two-phase
13 olive mill waste [19]. Experimental results showed that char yields from the olive mill waste
14 decreased with increasing pressure. The authors claim that the observed effects of pressure on
15 char yield are unexpected. The authors state that, with the amount of sample used in the TGA
16 experiments, contacts between studied sample particles and generated tarry vapors are rather
17 poor and insufficient for secondary char formation [19]. Further pressurized TGA experiments
18 were suggested, which should carefully consider factors (i.e., gas residence time, particle size
19 and sample mass) affecting diffusivity of the tarry vapors [19]. On the other hand, in the same
20 work, the highest fixed carbon yield was realized as the experiments were conducted at a higher
21 pressure.

22
23
24
25
26
27
28
29
30
31
32
33
34
35
36
37
38
39
40
41
42
43
44
45
46
47
48
49 In the present work, effects of pressure at constant volumetric flow rate on the char yields from
50 the studied biomasses were also examined. The volumetric flow rate of the purge gas is
51 associated with its superficial velocity. It means that residence time of pyrolysis vapors should
52 be similar for experiments carried out at elevated pressure and a constant volumetric flow rate.
53
54
55
56
57
58
59
60

1
2
3 Table 5 summarizes char yields and fixed carbon yields realized at two different pressures with
4 either constant mass flow rate or volumetric flow rate. The \pm values associated with represent the
5 sample standard deviation of three (for spruce and birch wood) to five (spruce and birch forest
6 residue) identical runs with the PTGA. It is clear to see that for the constant gas flow conditions,
7 increasing pressure favors char yield and fixed carbon yields for all studied samples.
8 Additionally, slightly higher char yields and fixed carbon yields were obtained from experiments
9 conducted at a constant mass flow rate. One should note that to maintain a constant volumetric
10 flow rate of the purge gas, increased gas mass flow is needed with increasing pressure. It might
11 result in decrease of partial pressures of the pyrolysis vapors, which affects char yields and fixed
12 carbon yields from the studied samples. These findings concerning change of char yields at
13 elevated pressures with either different or identical gas flow rates agree well with results
14 reported by Richard et al. [27]. They observed that char yields from cellulose in a
15 thermogravimetric analyzer was significantly enhanced at elevated pressures at either a constant
16 purge gas flow rate or a constant purge gas velocity. Increasing of pressure together with
17 constant purge gas mass flow rate gave more evident effects on char yields from cellulose [27].
18 Positive effects of pressure on char yield from different biomass materials were also observed as
19 they were pyrolyzed in batch reactors. In the last decades, Antal and coworkers reported evident
20 increase of both char and fixed carbon yields from various biomasses, as they were carbonized in
21 a flash carbonizer at a pressure from atmospheric to 0.5-3.0 MPa [11, 13, 16]. In another work,
22 eucalyptus wood samples were pyrolyzed in a pressurized reactor at two final temperatures (450
23 and 600 °C) and three pressures (0, 5 and 10 bars) [5]. The pressure had the most pronounced
24 effect on char yield at 450 °C. For eucalyptus wood samples with different moisture content, the
25 char yields increased from 33.2%-36.9% to 41.9%-43.5% as the pressure increased from 0 to 10
26
27
28
29
30
31
32
33
34
35
36
37
38
39
40
41
42
43
44
45
46
47
48
49
50
51
52
53
54
55
56
57
58
59
60

1
2
3 bar ^[5]. In addition, the fixed carbon yields were also significantly increased for those samples
4
5
6
7
8
9
10
11
12
13
14
15
16
17
18
19
20
21
22
23
24
25
26
27
28
29
30
31
32
33
34
35
36
37
38
39
40
41
42
43
44
45
46
47
48
49
50
51
52
53
54
55
56
57
58
59
60
pyrolyzed at higher pressures.

Table 6 displays the results of flash carbonization experiments conducted at University of Hawaii. The two experiments were carried out at similar superficial air velocities, which maintained similar vapor phase residence times in both the packed sample bed and the reactor as well. Again, increasing the pressure from 0.8 MPa to 2.2 MPa significantly enhanced char and fixed carbon yields of spruce wood from 24.1 wt% and 20.7 wt% to 35.5 wt% and 28.0 wt%, respectively. This finding corroborates the earlier work and confirms the importance of elevated pressure in the formation of char.

Figures 9 and 10 display two parity plots for comparing fixed carbon yields realized from experiments with the calculated theoretical yields based on the ultimate analysis given in Table 3. Such comparison can be used to assess the efficiencies of the various carbonization procedures described above. For the spruce wood and forest residue (Figure 9), carbonization of them in TGA TA Q5000, in an open pan, was least efficient, offering the lowest fixed carbon yields, as low as 43% and 49% of the theoretical values, respectively. The proximate analysis procedure realized higher carbonization efficiencies and 51% and 58% fixed carbon yields were obtained from spruce wood and forest residue, respectively. The carbonization efficiencies were further improved by using closed crucibles in the TGAs (MT TGA and PTGA), 63% and 70% for spruce wood and forest residue in the PTGA, respectively. Operating at elevated pressures, the PTGA realized efficiencies from 64% and 70% (at 0.8 MPa) to 73% and 74% (at 2.2 MPa), as respectively spruce wood and forest residue were carbonized in open crucibles. It is interesting to see that, for the 10 mg spruce wood sample, 64% of the theoretical fixed carbon yield obtained in the PTGA in an open crucible at 0.8 MPa is close to that realized by employing a closed crucible

1
2
3 at 0.1 MPa (63%). The similarity in efficiencies were also observed for spruce forest residue as it
4 was carbonized at the same conditions. The fixed carbon yields from spruce wood and forest
5 residue were further improved as they were carbonized at 2.2 MPa and in closed crucibles, to
6 82% and 79% of the theoretical yields, respectively. The highest fixed carbon yield realized in
7 the present work was delivered by carbonizing spruce wood chips in the flash carbonizer at 2.2
8 MPa, approaching 85% of the theoretical yield. As shown in Figure 10, employing closed
9 crucibles and increased pressures enhanced carbonization efficiencies as also birch wood and
10 forest residue were carbonized with different procedures. The trends shown in the parity plots in
11 Figures 9 and 10 are in good agreement with our earlier work ^[10, 12].
12
13
14
15
16
17
18
19
20
21
22
23
24

25 3.5 SEM images of char produced under various conditions

26
27 Figure 11 displays SEM images of spruce wood and forest residue char samples produced in the
28 PTGA at 950 °C and 0.1 MPa in open crucibles. The char particles can be easily distinguished as
29 discrete particles as shown in Figure 11. As can be seen, the typical spruce wood char particles
30 are oblong solid thick particles and thin fibres like particles. The fibrous particles are rarely
31 found from the SEM image of spruce forest residue char shown in Figure 11-b. In addition, there
32 are particles with more spherical shape and indented contour as can be seen in Figure 11-b. For
33 most char particles shown in Figure 11, the surfaces are rather clean and smooth. Figures 12 and
34 13 show representative SEM images of spruce wood and forest residue char produced at 950 °C
35 and 2.2 MPa in closed crucibles. Figures 12 a and b show spruce wood char from two
36 experiments under identical conditions (i.e., with 2.2 MPa pressure and closed crucible). It was
37 observed that the char have aggregated together to form a dense bulk structure. In addition, there
38 are significant amounts of deposits on the char particle surfaces. This is very different compared
39 to char residues collected in open crucibles after pyrolyzing at atmospheric pressure. Figure 13-a
40
41
42
43
44
45
46
47
48
49
50
51
52
53
54
55
56
57
58
59
60

1
2
3 and b displays more evident agglomeration of spruce forest residue char produced from a 2.2
4 MPa pressure and closed crucible experiment. The char particles have lost their own identities
5 and particles with an original structure and shape are not visible. Figure 12 c-e and Figure 13 c-e
6
7
8 show zoom in view of deposits on surfaces of spruce wood and forest residue char particles by
9
10 increasing magnifications. These deposits have smooth surfaces and are more transparent,
11
12 indicating different chemical composition of them compared to the bulk of the char particle. In
13
14 addition, Figure 14 shows that some spruce forest residue char particles lost their tubular
15
16 structure with formation of a more smooth and intact surface. The differences in microstructure
17
18 and morphology between char particles produced under different conditions can be assigned to
19
20 effects of pressure and confinement of pyrolysis products. Figures 15 and 16 show spruce wood
21
22 char that passed a molten stage during carbonization at elevated pressure. The melting and
23
24 swelling of spruce wood and forest residue char particles presented in this work agree well with
25
26 findings reported in our previous work and other studies ^[10, 47, 48]. Wood materials are cellular
27
28 substance with vessel structure and evident cavities. During a carbonization process, volatile
29
30 products due to the devolatilization of the wood experience pressure-driven flow through the
31
32 wood vessel and tubular structures. At elevated pressure, melting of cell structure and
33
34 recondensation/deposition of secondary carbon are more intensive, causing a porosity blockage
35
36 in wood char particles. Blockage and accumulation of volatile products inside the wood char
37
38 cause expansion and damage of the tubular structure as shown in Figure 15 c and d. Figure 16
39
40 displays severe swelling of one char particle due to evacuation of volatile products as the sample
41
42 is in its molten state. It results in complete loss of original tubular structure and formation of
43
44 large holes. At elevated pressures, residence time of volatile products from the interior of the
45
46 wood particles is prolonged. In addition, loss of porosity and closing of openings of the char
47
48
49
50
51
52
53
54
55
56
57
58
59
60

1
2
3 particles will further extend the residence time of volatile products inside the char matrix. Thus,
4
5 heterogeneous secondary reactions of tarry vapours have more opportunities to occur, leading to
6
7 formation of secondary char and increase of both char and fixed carbon yields.
8
9

10 11 12 **4 CONCLUSIONS**

13
14 In the present work, effects of process conditions including vapor residence time, sample size
15
16 and pressure on char and fixed carbon yields of spruce stem wood, spruce forest residue, birch
17
18 stem wood and birch forest residue were studied. Below is major conclusions and findings
19
20 obtained.
21
22

- 23
24
25 • Extending of the vapor residence time can improve the char and fixed carbon yields
26
27 determined by TGA. For the four ground samples, carbonization TGAs at atmospheric
28
29 pressure in open pans offered the lowest fixed carbon yields (~ 40% to 48% of theoretical
30
31 values). Slightly higher char and fixed carbon yields were realized by using deep and
32
33 narrow crucibles that isolate samples from the purge gas flow. Moreover, using a closed
34
35 crucible considerably improved char and fixed carbon yields as measured by TGA. As
36
37 one studied sample is carbonized in either deep/narrow or closed crucible, the release of
38
39 pyrolysis volatiles is restricted and residence time of them in the solid char is prolonged
40
41 It enhances contacts of vapor phases with solid char and secondary pyrolysis reactions
42
43 and augment of char and fixed carbon yield consequently.
44
45
46
47
- 48
49 • The char and fixed carbon yields determined by TGAs were considerably affected by
50
51 sample particle size. For TGA experiments conducted at 0.1 MPa using open crucibles,
52
53 an increase of the birch forest residue particle size from $0.063 < d < 0.125$ mm to < 1 mm
54
55 resulted in increases of char yield at 950 °C from 17 wt% to 23 wt%. The influence of
56
57
58
59
60

1
2
3 sample particle size on char yield was more pronounced as experiments were performed
4
5 under elevated pressures. Compared to small particles, the residence time of pyrolytic
6
7 vapors in the larger particles is longer, which have more intensive contact with the
8
9 nascent char solid matrix. The pyrolytic vapors might crack into solid and gases with
10
11 presence of solid charcoal surface, resulting in increased char yield consequently.
12
13
14
15

- 16 • Increasing of pressure gave the most pronounced enhancement of char and fixed carbon
17
18 yields of the four studied woody biomasses. Especially noteworthy are increases in char
19
20 yields of spruce wood and forest residue, which increased from 19 wt% and 24 wt% to 26
21
22 wt% and 33 wt%, respectively, with an increase of pressure from 0.1 MPa to 2.2 MPa (at
23
24 a constant mass flow rate). Increasing of pressure with a constant volumetric flow rate
25
26 also enhanced char and fixed carbon yields from the studied woody biomass samples. In
27
28 the present work, the highest char yield (35.5 wt%) was obtained from carbonization of
29
30 spruce wood in the flash carbonization reactor. The experimental fixed carbon yield
31
32 approaches 85% of the theoretical value.
33
34
35
36
37
- 38 • The SEM analyses revealed evident differences in morphology and microstructure of
39
40 char residues produced from the studied woody biomasses at different conditions. After
41
42 pyrolyzed at 950°C and 2.2. MPa in closed crucibles, the spruce wood and forest residue
43
44 char particles started to agglomerate together with more a compact structure. In addition,
45
46 there is formation of deposits on surfaces of char particles, which have smooth and intact
47
48 surface and might be associated with recondensation of tarry vapors. The spruce wood
49
50 char produced in the flash carbonization reactor experienced a molten stage, with
51
52 observation of large holes and small bubbles from char particles as well.
53
54
55
56
57
58
59
60

- 1
2
3
4
5
6
7
8
9
10
11
12
13
14
15
16
17
18
19
20
21
22
23
24
25
26
27
28
29
30
31
32
33
34
35
36
37
38
39
40
41
42
43
44
45
46
47
48
49
- The results presented in this work imply that conditions (i.e., increasing pressure, confinement of tarry vapors and large particle size) improving or augmenting contacts between carbonization vapor phases with the solid char matrix can considerably enhance char and fixed carbon yield from the studied woody biomasses. Therefore, measures that can help to realize these conditions can be considered and implemented in industry processes for increasing char yield and quality (i.e., fixed carbon content) of the charcoal product. In addition, properties of the final charcoal product will be different, as the carbonization process is carried out under conditions (i.e., pressurized) different than conventional conditions. Further work is needed to characterize and assess charcoal produced under varied conditions, for use in different final applications.
 - For woody biomass, size reduction by shredding and grinding consumes significant energy and is labor and capital intensive. Moreover, as shown in the present work, size reduction cause decrease of char and fixed carbon yields in the produced charcoal from the studied woody biomasses. With these considerations, as charcoal is a desired product, size reduction is not necessary or even futile. High yield and quality charcoal can be produced from the woody biomasses without intensive size reduction. It gives a carbonization process a great advantage over other thermochemical conversion processes with aim to convert woody biomasses into high value fuels.

50 ACKNOWLEDGMENT

51
52 The authors acknowledge the financial support by the Research Council of Norway and a
53 number of industrial partners through the project BioCarb+ (“Enabling the biocarbon value chain
54 for energy”).
55
56
57
58
59
60

REFERENCES

1. Antal Jr MJ, Grønli M. The art, science, and technology of charcoal production. *Industrial and Engineering Chemistry Research*. 2003;42(8):1619-40.
2. Tripathi M, Sahu JN, Ganesan P. Effect of process parameters on production of biochar from biomass waste through pyrolysis: A review. *Renewable and Sustainable Energy Reviews*. 2016;55:467-81.
3. Manyà JJ. Pyrolysis for Biochar Purposes: A Review to Establish Current Knowledge Gaps and Research Needs. *Environmental Science & Technology*. 2012;46(15):7939-54.
4. Wang L, Várhegyi G, Skreiberg Ø, Li T, Grønli M, Antal MJ. Combustion Characteristics of Biomass Charcoals Produced at Different Carbonization Conditions: A Kinetic Study. *Energy & Fuels*. 2016;30(4):3186-97.
5. Rousset P, Figueiredo C, De Souza M, Quirino W. Pressure effect on the quality of eucalyptus wood charcoal for the steel industry: A statistical analysis approach. *Fuel Processing Technology*. 2011;92(10):1890-7.
6. Abdullah H, Wu H. Biochar as a Fuel: 1. Properties and Grindability of Biochars Produced from the Pyrolysis of Mallee Wood under Slow-Heating Conditions. *Energy & Fuels*. 2009;23(8):4174-81.
7. Abdullah H, Mediaswanti KA, Wu H. Biochar as a Fuel: 2. Significant Differences in Fuel Quality and Ash Properties of Biochars from Various Biomass Components of Mallee Trees. *Energy & Fuels*. 2010;24(3):1972-9.
8. Suopajarvi H, Pongrácz E, Fabritius T. The potential of using biomass-based reducing agents in the blast furnace: A review of thermochemical conversion technologies and assessments related to sustainability. *Renewable and Sustainable Energy Reviews*. 2013;25:511-28.
9. Agrados A, De Marco I, López-Uriónabarrenechea A, Solar J, Caballero BM, Gastelu N. Biomass pyrolysis solids as reducing agents: Comparison with commercial reducing agents. *Materials*. 2016;9(1).
10. Wang L, Skreiberg O, Gronli M, Specht GP, Antal MJ. Is elevated pressure required to achieve a high fixed-carbon yield of charcoal from biomass? Part 2: The importance of particle size. *Energy and Fuels*. 2013;27(4):2146-56.
11. Antal Jr MJ, Allen SG, Dai X, Shimizu B, Tam MS, Grønli M. Attainment of the theoretical yield of carbon from biomass. *Industrial and Engineering Chemistry Research*. 2000;39(11):4024-31.
12. Wang L, Trninic M, Skreiberg Ø, Gronli M, Considine R, Antal MJ. Is Elevated Pressure Required To Achieve a High Fixed-Carbon Yield of Charcoal from Biomass? Part 1: Round-Robin Results for Three Different Corn cob Materials. *Energy & Fuels*. 2011;25(7):3251-65.
13. Antal Jr MJ, Mochizuki K, Paredes LS. Flash carbonization of biomass. *Industrial and Engineering Chemistry Research*. 2003;42(16):3690-9.
14. Yoshida T, Antal Jr MJ, editors. Flash carbonization of sewage sludge: Assessment of sewage sludge charcoal land application. *AIChE Annual Meeting, Conference Proceedings*; 2008.
15. Antal MJ, Mok WSL, Varhegyi G, Szekely T. Review of methods for improving the yield of charcoal from biomass. *Energy & Fuels*. 1990;4(3):221-5.
16. Antal MJ, Croiset E, Dai X, DeAlmeida C, Mok WS-L, Norberg N, et al. High-Yield Biomass Charcoal. *Energy & Fuels*. 1996;10(3):652-8.
17. Antal MJ, Nunoura T, Wade S, editors. Optimization of flash carbonization(Tm) conditions for charcoal production from sunflower shells. *AIChE Annual Meeting, Conference Proceedings*; 2006.
18. Van Wesenbeeck S, Higashi C, Legarra M, Wang L, Antal MJ. Biomass Pyrolysis in Sealed Vessels. Fixed-Carbon Yields from Avicel Cellulose That Realize the Theoretical Limit. *Energy & Fuels*. 2016;30(1):480-91.
19. Manyà JJ, Laguarda S, Ortigosa MA, Manso JA. Biochar from Slow Pyrolysis of Two-Phase Olive Mill Waste: Effect of Pressure and Peak Temperature on its Potential Stability. *Energy & Fuels*. 2014;28(5):3271-80.
20. Manyà JJ, Ortigosa MA, Laguarda S, Manso JA. Experimental study on the effect of pyrolysis pressure, peak temperature, and particle size on the potential stability of vine shoots-derived biochar. *Fuel*. 2014;133(0):163-72.
21. Manyà JJ, Roca FX, Perales JF. TGA study examining the effect of pressure and peak temperature on biochar yield during pyrolysis of two-phase olive mill waste. *Journal of Analytical and Applied Pyrolysis*. 2013;103(0):86-95.
22. Demirbas A. Effects of temperature and particle size on bio-char yield from pyrolysis of agricultural residues. *Journal of Analytical and Applied Pyrolysis*. 2004;72(2):243-8.
23. Budai A, Wang L, Gronli M, Strand LT, Antal MJ, Abiven S, et al. Surface properties and chemical composition of corn cob and miscanthus biochars: Effects of production temperature and method. *Journal of Agricultural and Food Chemistry*. 2014;62(17):3791-9.
24. Mok WSL, Antal Jr MJ. Effects of pressure on biomass pyrolysis. I. Cellulose pyrolysis products. *Thermochimica Acta*. 1983;68(2-3):155-64.

- 1
 - 2
 - 3
 - 4
 - 5
 - 6
 - 7
 - 8
 - 9
 - 10
 - 11
 - 12
 - 13
 - 14
 - 15
 - 16
 - 17
 - 18
 - 19
 - 20
 - 21
 - 22
 - 23
 - 24
 - 25
 - 26
 - 27
 - 28
 - 29
 - 30
 - 31
 - 32
 - 33
 - 34
 - 35
 - 36
 - 37
 - 38
 - 39
 - 40
 - 41
 - 42
 - 43
 - 44
 - 45
 - 46
 - 47
 - 48
 - 49
 - 50
 - 51
 - 52
 - 53
 - 54
 - 55
 - 56
 - 57
 - 58
 - 59
 - 60
25. Mok WSL, Antal Jr MJ. Effects of pressure on biomass pyrolysis. II. Heats of reaction of cellulose pyrolysis. *Thermochimica Acta*. 1983;68(2-3):165-86.
26. Antal MJ, Jr., Varhegyi G. Cellulose Pyrolysis Kinetics: The Current State of Knowledge. *Industrial & Engineering Chemistry Research*. 1995;34(3):703-17.
27. Richard J-R, Antal MJ. Thermogravimetric Studies of Charcoal Formation from Cellulose at Elevated Pressures. In: Bridgwater AV, editor. *Advances in Thermochemical Biomass Conversion*. Dordrecht: Springer Netherlands; 1993. p. 784-92.
28. Nunoura T, Wade SR, Bourke JP, Antal Jr MJ. Studies of the flash carbonization process. I. Propagation of the flaming pyrolysis reaction and performance of a catalytic afterburner. *Industrial and Engineering Chemistry Research*. 2006;45(2):585-99.
29. Williams S, Higashi C, Phothisantikul P, Wesenbeeck SV, Antal Jr MJ. The fundamentals of biocarbon formation at elevated pressure: From 1851 to the 21st century. *Journal of Analytical and Applied Pyrolysis*. 2015;113:225-30.
30. Di Blasi C. Modeling chemical and physical processes of wood and biomass pyrolysis. *Progress in Energy and Combustion Science*. 2008;34(1):47-90.
31. Di Blasi C, Branca C, Lombardi V, Ciappa P, Di Giacomo C. Effects of Particle Size and Density on the Packed-Bed Pyrolysis of Wood. *Energy & Fuels*. 2013;27(11):6781-91.
32. Werkelin J, Lindberg D, Boström D, Skrifvars B-J, Hupa M. Ash-forming elements in four Scandinavian wood species part 3: Combustion of five spruce samples. *Biomass and Bioenergy*. 2011;35(1):725-33.
33. Wang L, Dibdiakova J. Characterization of Ashes from Different Wood Parts of Norway Spruce Tree. *Chemical Engineering Transactions*. 2014;37:37-42.
34. Reynolds WC. STANJAN Thermochemical Equilibrium. Software, 391 ed. Stanford University: Stanford, CA, :1987.
35. Bennadji H, Smith K, Serapiglia MJ, Fisher EM. Effect of Particle Size on Low-Temperature Pyrolysis of Woody Biomass. *Energy & Fuels*. 2014;28(12):7527-37.
36. Haykiri-Acma H. The role of particle size in the non-isothermal pyrolysis of hazelnut shell. *Journal of Analytical and Applied Pyrolysis*. 2006;75(2):211-6.
37. Mani T, Murugan P, Abedi J, Mahinpey N. Pyrolysis of wheat straw in a thermogravimetric analyzer: Effect of particle size and heating rate on devolatilization and estimation of global kinetics. *Chemical Engineering Research and Design*. 2010;88(8):952-8.
38. Pattanotai T, Watanabe H, Okazaki K. Experimental investigation of intraparticle secondary reactions of tar during wood pyrolysis. *Fuel*. 2013;104:468-75.
39. Shen J, Wang X-S, Garcia-Perez M, Mourant D, Rhodes MJ, Li C-Z. Effects of particle size on the fast pyrolysis of oil mallee woody biomass. *Fuel*. 2009;88(10):1810-7.
40. Asadullah M, Zhang S, Li C-Z. Evaluation of structural features of chars from pyrolysis of biomass of different particle sizes. *Fuel Processing Technology*. 2010;91(8):877-81.
41. Zobel N, Anca-Couce A. Slow pyrolysis of wood particles: Characterization of volatiles by Laser-Induced Fluorescence. *Proceedings of the Combustion Institute*. 2013;34(2):2355-62.
42. Zobel N, Anca-Couce A. Influence of intraparticle secondary heterogeneous reactions on the reaction enthalpy of wood pyrolysis. *Journal of Analytical and Applied Pyrolysis*. 2015;116:281-6.
43. Antal MJ, Jr., Helsen LM, Kouzu M, Lédé J, Matsumura Y. Rules of thumb (Empirical Rules) for the biomass utilization by thermochemical conversion. *Nihon Enerugi Gakkaiishi/Journal of the Japan Institute of Energy*. 2014;93(8):684-702.
44. Li C-Z. Importance of volatile-char interactions during the pyrolysis and gasification of low-rank fuels – A review. *Fuel*. 2013;112(0):609-23.
45. Okuno T, Sonoyama N, Hayashi J-i, Li C-Z, Sathe C, Chiba T. Primary Release of Alkali and Alkaline Earth Metallic Species during the Pyrolysis of Pulverized Biomass. *Energy & Fuels*. 2005;19(5):2164-71.
46. Sun CL, Xiong YQ, Liu QX, Zhang MY. Thermogravimetric study of the pyrolysis of two Chinese coals under pressure. *Fuel*. 1997;76(7):639-44.
47. Biagini E, Narducci P, Tognotti L. Size and structural characterization of lignin-cellulosic fuels after the rapid devolatilization. *Fuel*. 2008;87(2):177-86.
48. Cetin E, Moghtaderi B, Gupta R, Wall TF. Influence of pyrolysis conditions on the structure and gasification reactivity of biomass chars. *Fuel*. 2004;83(16):2139-50.
49. Raveendran K, Ganesh A, Khilar KC. Influence of mineral matter on biomass pyrolysis characteristics. *Fuel*. 1995;74(12):1812-22.

- 1
2
3 50. Nik-Azar M, Hajaligol MR, Sohrabi M, Dabir B. Mineral matter effects in rapid pyrolysis of beech wood.
4 Fuel Processing Technology. 1997;51(1):7-17.
5 51. Hu S, Jiang L, Wang Y, Su S, Sun L, Xu B, et al. Effects of inherent alkali and alkaline earth metallic
6 species on biomass pyrolysis at different temperatures. Bioresource Technology. 2015;192:23-30.
7
8
9
10
11
12
13
14
15
16
17
18
19
20
21
22
23
24
25
26
27
28
29
30
31
32
33
34
35
36
37
38
39
40
41
42
43
44
45
46
47
48
49
50
51
52
53
54
55
56
57
58
59
60

Table 1 Specifications of Instruments and Crucible/pan

Instruments	Crucible/pan volume(μ l)	Crucible/pan geometry ($d \times h$, mm)
TA Q5000	pan (90 μ l)	10 x 1
PTGA	crucible (120 μ l)	6 x 4.5
MT TGA	crucible (150 μ l)	7 x 4.5
MT TGA	crucible (900 μ l)	12 x 16

Table 2. Table 2. Proximate Analysis, Fixed Carbon Yield, Heating value, and Inorganic Elements Concentrations of Feed Materials

	Proximate analysis (wt%) ^a				HHV	Ash forming elements (mg/kg)							
	VM	fC	ash	y_{fC} (wt%)	MJ/kg	Si	Ca	K	Na	P	Mg	Fe	Mn
Spruce wood	82.53	16.91	0.56	17.0	19.64	63	1948	672	42	61	212	39	323
Spruce forest residue	76.31	21.19	2.5	21.7	20.63	571	6004	2516	48	349	649	113	877
Birch wood	84.43	14.79	0.78	14.9	19.57	125	2109	725	22	165	314	118	162
Birch forest residue	79.14	18.21	2.65	18.7	20.83	409	5022	2002	42	543	770	317	342

^a Dry mass basis.Table 3. Ultimate Analysis of Feed Materials and Calculated Theoretical Fixed Carbon Yield, y_{fC}

	Ultimate analysis (wt%) ^a					
	C	H	O ^b	N	S	y_{fC} (wt%)
Spruce wood	49.64	6.40	43.81	0.13	0.02	33.6
Spruce forest residue	51.66	6.13	41.49	0.68	0.04	37.5
Birch wood	49.94	6.72	43.06	0.26	0.02	33.7
Birch forest residue	50.74	6.32	42.06	0.84	0.04	35.3

^a Dry mass basis. ^b Oxygen content calculated by difference.

Table 4. Proximate Analysis, Char and Fixed Carbon Yields Realized at Atmospheric Pressure (0.1 MPa) in the MT TGA

Sample	TGA exp	Proximate analysis (wt%) ^a				
		VM	fC	ash	y_{char} (wt%) ^b	y_{fC} (wt%) ^b
Spruce wood 100 mg	open crucible	4.04	94.97	0.99	22.3 \pm 0.2	21.3 \pm 0.1
Spruce wood 100 mg	closed crucible	4.28	92.92	2.8	24.1 \pm 0.2	22.6 \pm 0.1
Spruce forest residue 100 mg	open crucible	8.99	85.39	5.62	28.7 \pm 0.7	24.5 \pm 0.5
Spruce forest residue 100 mg	closed crucible	8.19	85.06	6.75	30.8 \pm 0.5	26.5 \pm 0.3
Birch wood 100 mg	open crucible	6.04	92.67	1.29	18.2 \pm 0.2	17.0 \pm 0.1
Birch wood 100 mg	closed crucible	6.11	90.29	3.60	21.9 \pm 0.2	19.9 \pm 0.1
Birch forest residue 100 mg	open crucible	9.43	84.65	5.92	26.6 \pm 0.6	22.5 \pm 0.4
Birch forest residue 100 mg	closed crucible	9.56	83.49	6.95	28.7 \pm 0.4	24.2 \pm 0.3

^a ASTM E1131-08, ^b The \pm values associated with represent the sample standard deviation of three (for spruce and birch wood) to five (spruce and birch forest residue) identical runs with the MT TGA

Table 5. Char and Fixed Carbon Yields Realized at Elevated Pressure in PTGA at Constant Volumetric Flow Rate and Constant Mass Flow Rate

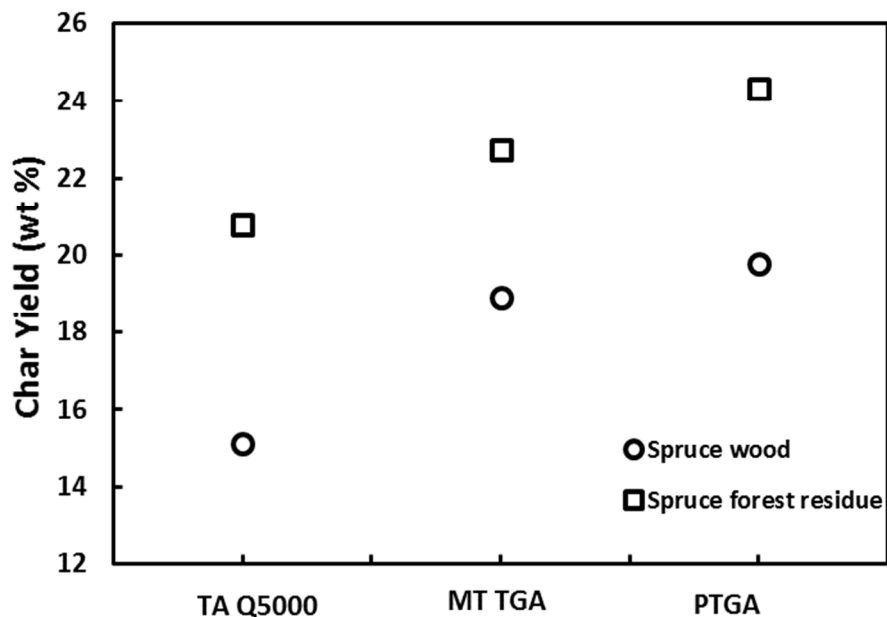
	y_{char} (wt%) ^a				y_{FC} (wt%) ^b			
	0.8 MPa ^c	0.8 MPa ^d	2.2 MPa ^c	2.2 MPa ^d	0.8 MPa ^c	0.8 MPa ^d	2.2 MPa ^c	2.2 MPa ^d
Spruce wood	20.9±0.5	22.5±0.3	24.0±0.4	25.7±0.2	20.0±0.4	21.5±0.2	22.9±0.2	24.6±0.1
Spruce forest residue	29.0±1	30.9±0.6	30.4±1.0	32.5±0.7	24.8±0.8	26.5±0.5	26.0±0.8	27.9±0.6
Birch wood	18.1±0.4	19.0±0.2	20.0±0.5	21.2±0.6	16.9±0.3	17.8±0.1	18.7±0.4	19.8±0.4
Birch forest residue	24.3±0.9	25.9±0.7	26.3±1.2	28.5±0.8	21.1±0.7	22.5±0.6	24.8±1.1	22.9±0.6

^a Percent of dry feed material. ^b $y_{\text{FC}} = \text{char yield} \times (100 - \% \text{ volatile matter} - \% \text{ char ash}) / (100 - \% \text{ feed ash})$. The volatile matter for char produced at 950 °C and ash content measured from the charcoal produced in the MT TGA with 100 mg sample. ^c Realized at constant volumetric flow rate. ^d Realized at constant mass flow rate. The ± values associated with represent the sample standard deviation of three (for spruce and birch wood) to five (spruce and birch forest residue) identical runs with the PTGA

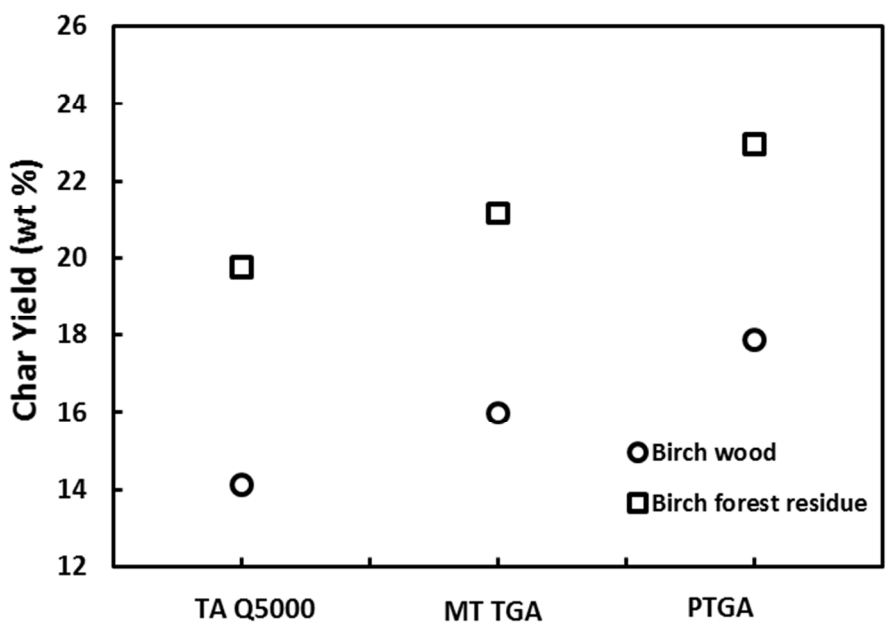
Table 6. Proximate analysis, Char and Fixed Carbon Yields Realized at Elevated Pressure in the FC Reactor

ID	Reactor pressure	Superficial velocity (mm/s)	Proximate analysis (wt%) ^a			y_{char} (wt%)	y_{FC} (wt%)
			VM	fC ^b	ash		
Spruce wood 150506	0.79	5.5	13.0	85.8	1.2	24.1	20.7
Spruce wood 150409	2.17	5.0	20.4	78.6	1.0	35.5	28.0

^a ASTM E1762-84



25 **Figure 1.** Effects of different instruments on spruce wood and spruce forest residue char yield in
26 an open crucible/pan.
27



49 **Figure 2.** Effects of different instruments on birch wood and birch forest residue char yield in
50 an open crucible/pan.
51
52
53
54
55
56
57
58
59
60

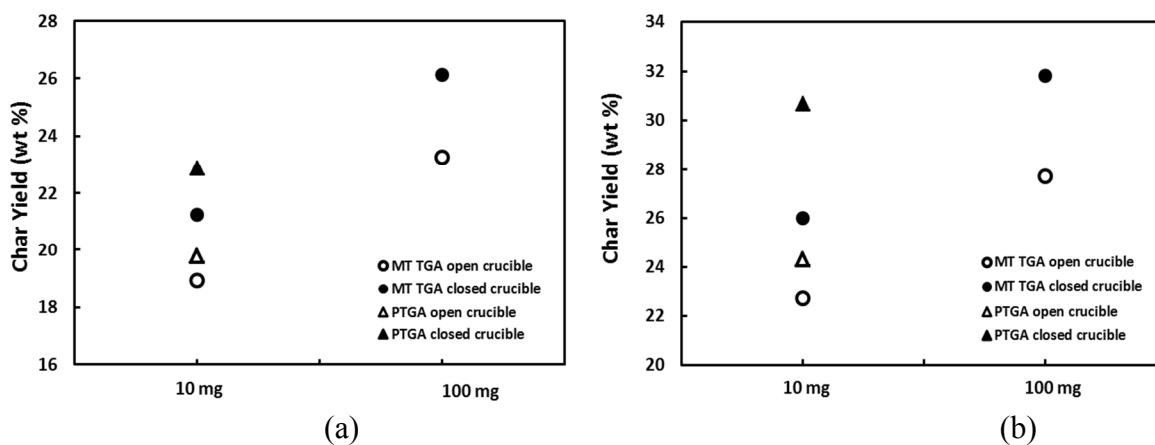


Figure 3. Effects of open vs. closed crucible and sample mass on (a) spruce wood and (b) spruce forest residue char yield.

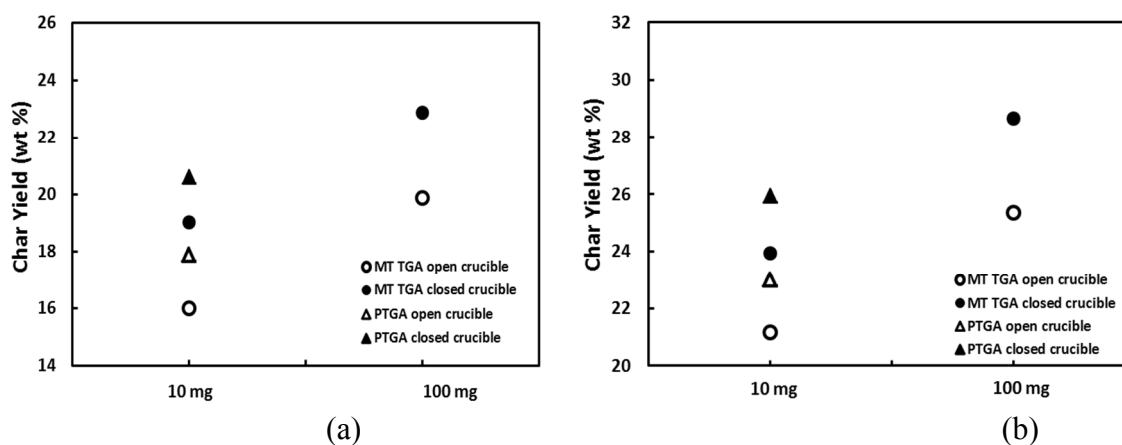
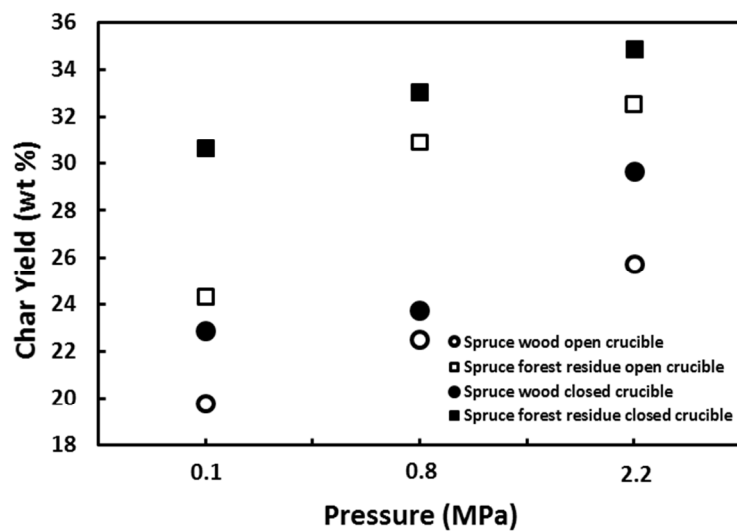
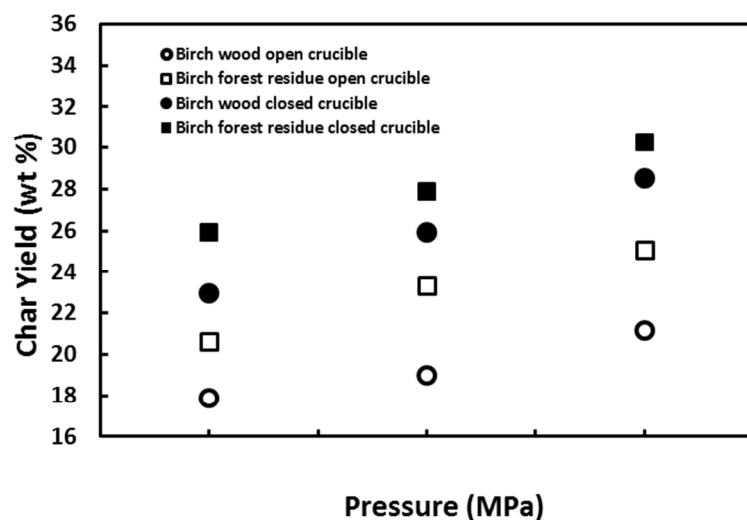


Figure 4. Effects of open vs. closed crucible and sample mass on (a) birch wood and (b) birch forest residue char yield.



21 **Figure 5.** Effects of pressure on spruce wood and spruce forest residue char yield.



43 **Figure 6.** Effects of pressure on birch wood and birch forest residue char yield.

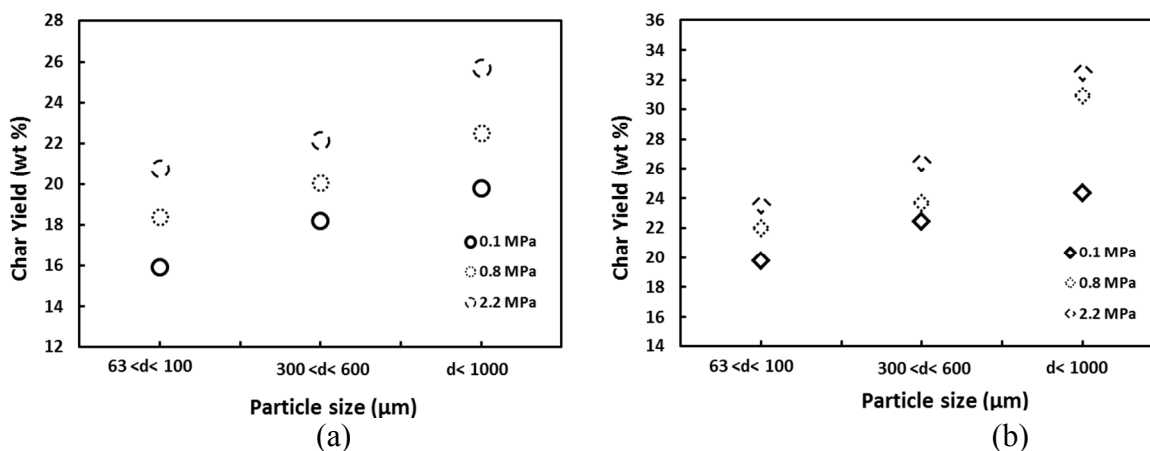


Figure 7. Influence of particle size and pressure on (a) spruce wood and (b) spruce forest residue char yield.

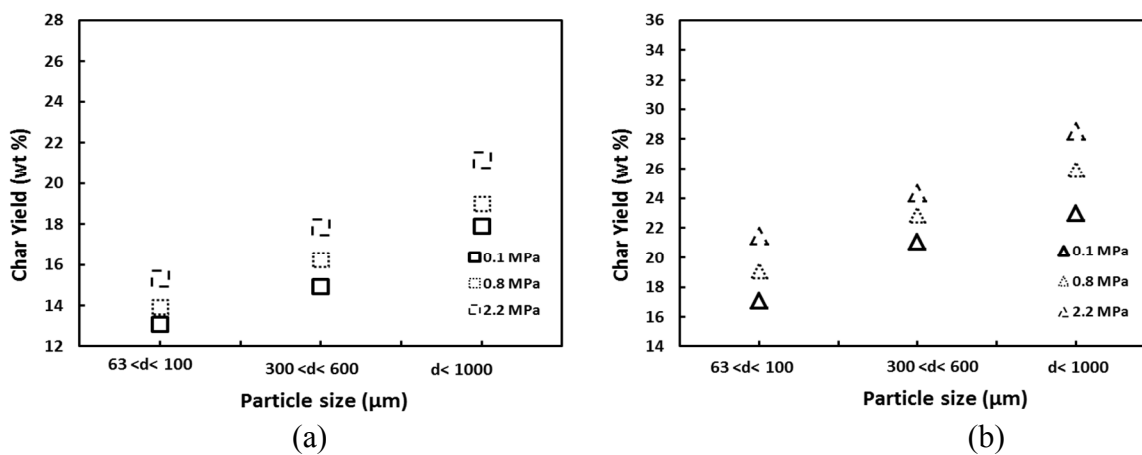


Figure 8. Influence of particle size and pressure on (a) birch wood and (b) birch forest residue char yield.

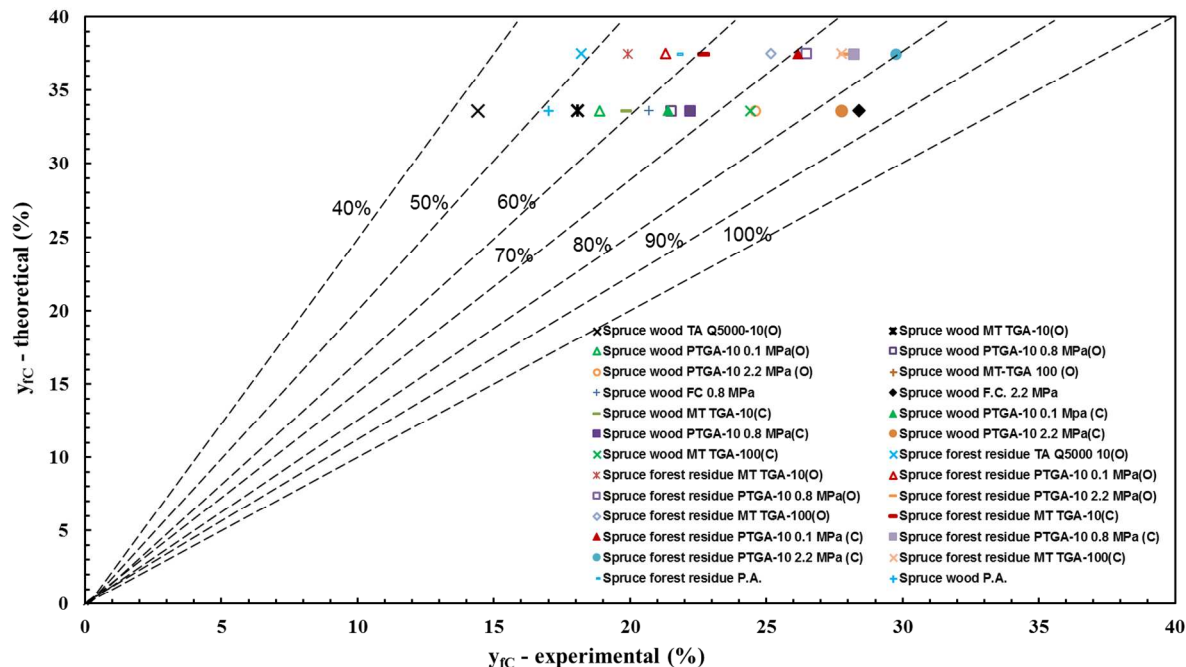


Figure 9. Parity plot displaying the Proximate Analysis (P.A.), Flash Carbonization (F.C.) and thermogravimetric analysis (TGA) of spruce wood and spruce forest residue with open and closed crucibles (o, c) at various pressures experimental fixed carbon yields vs. the theoretical values calculated using the ultimate elemental analyses given in Table 3.

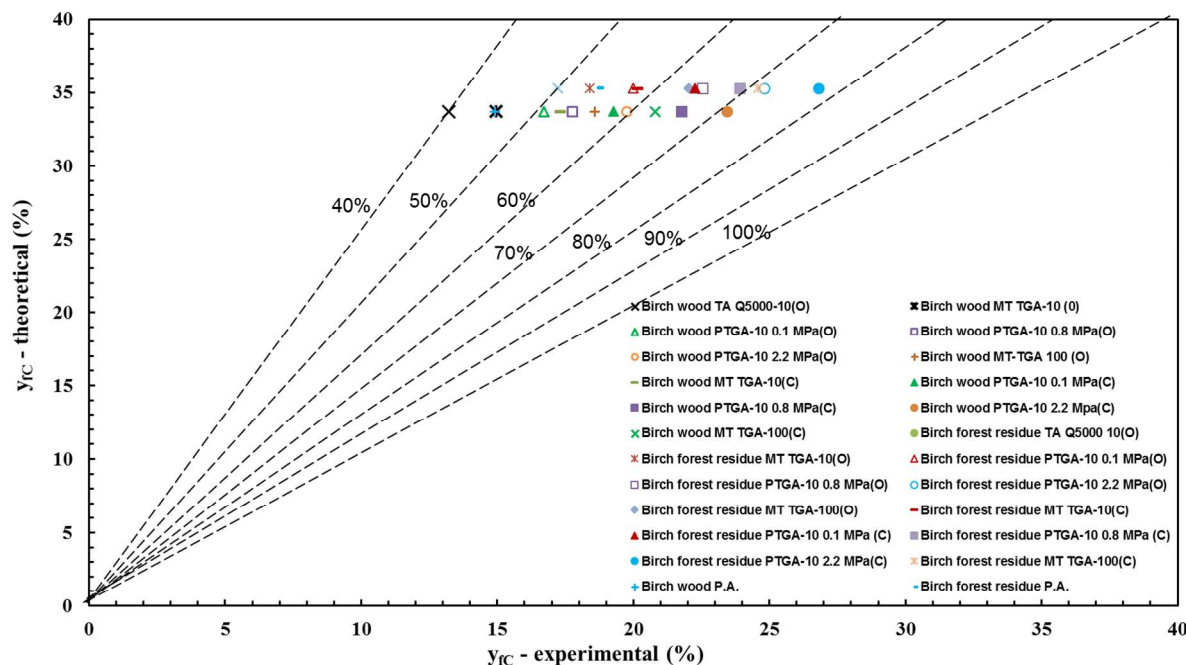


Figure 10. Parity plot displaying the Proximate Analysis (P.A.) and thermogravimetric analysis (TGA) of birch wood and birch forest residue with open and closed crucibles (o, c) at various

pressures experimental fixed carbon yields vs. the theoretical values calculated using the ultimate elemental analyses given in Table 3.

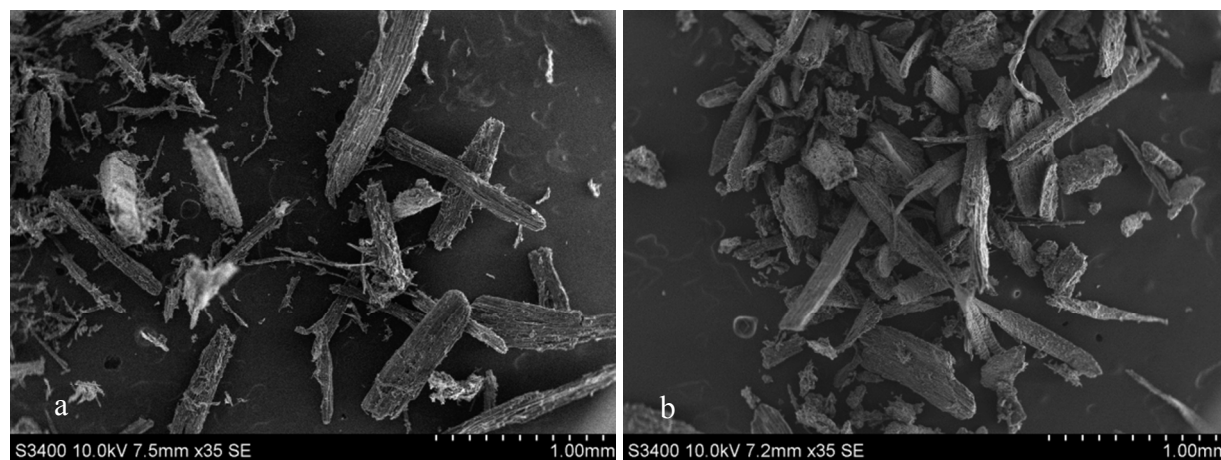


Figure 11. SEM micrographs of (a) spruce wood charcoal and (b) spruce forest residue charcoal produced in the PTGA at 0.1 MPa in open crucible

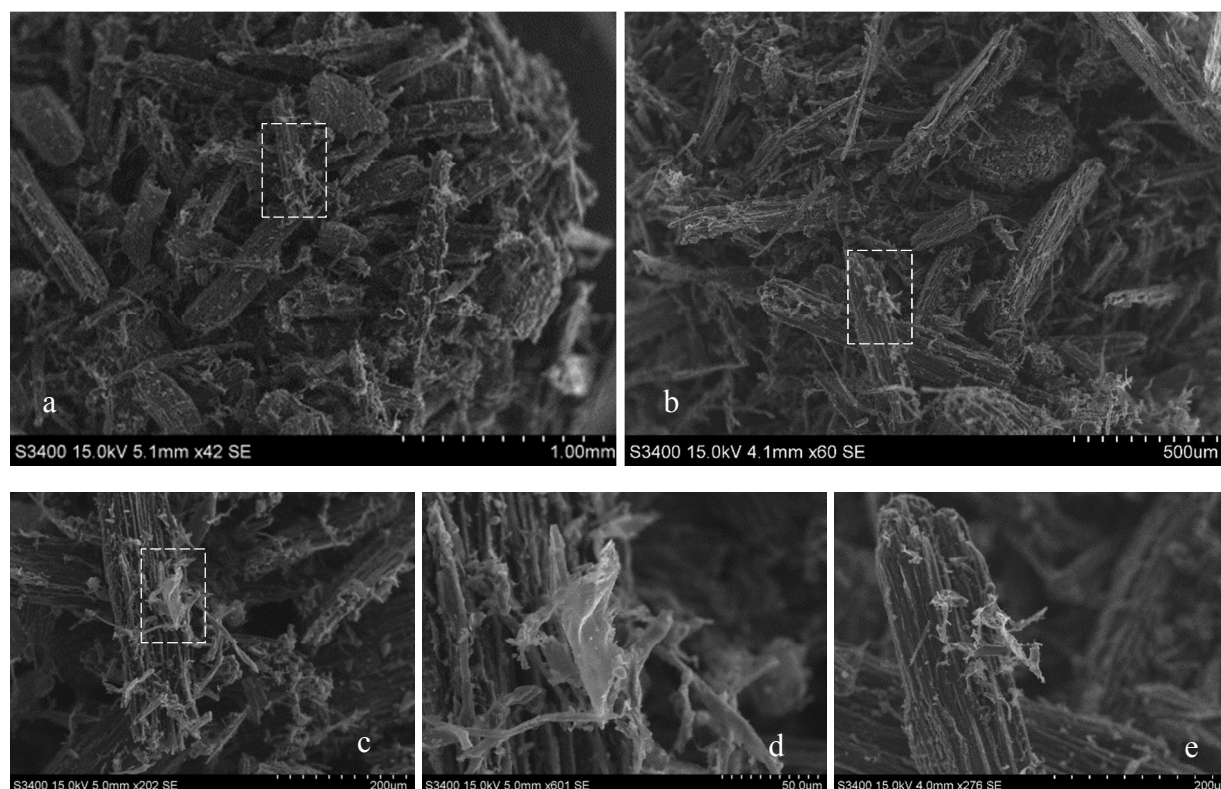
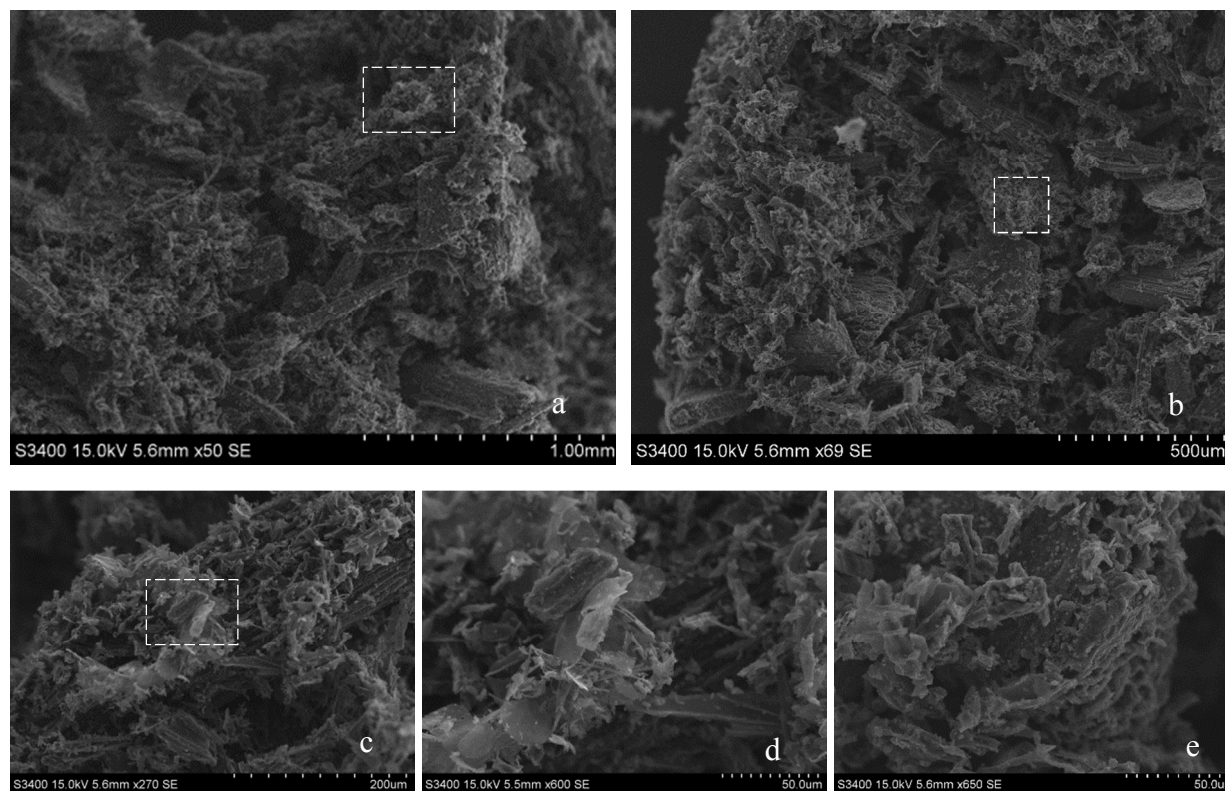
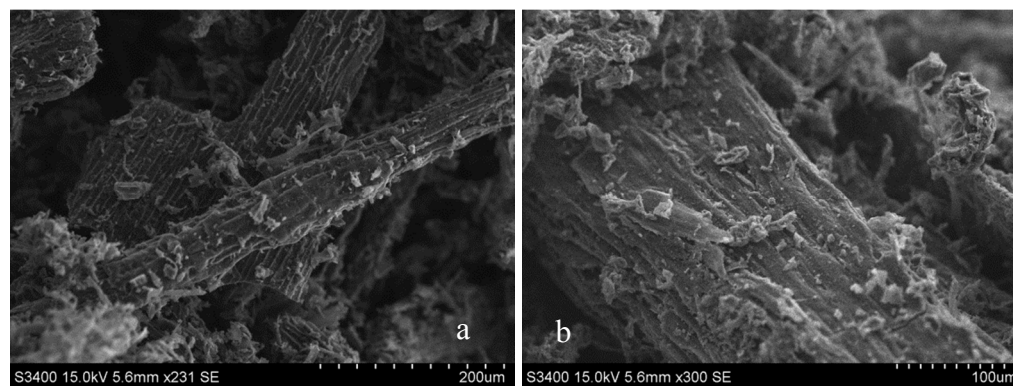


Figure 12. SEM micrographs of spruce wood charcoal produced in the PTGA in closed crucible at 2.2 MPa



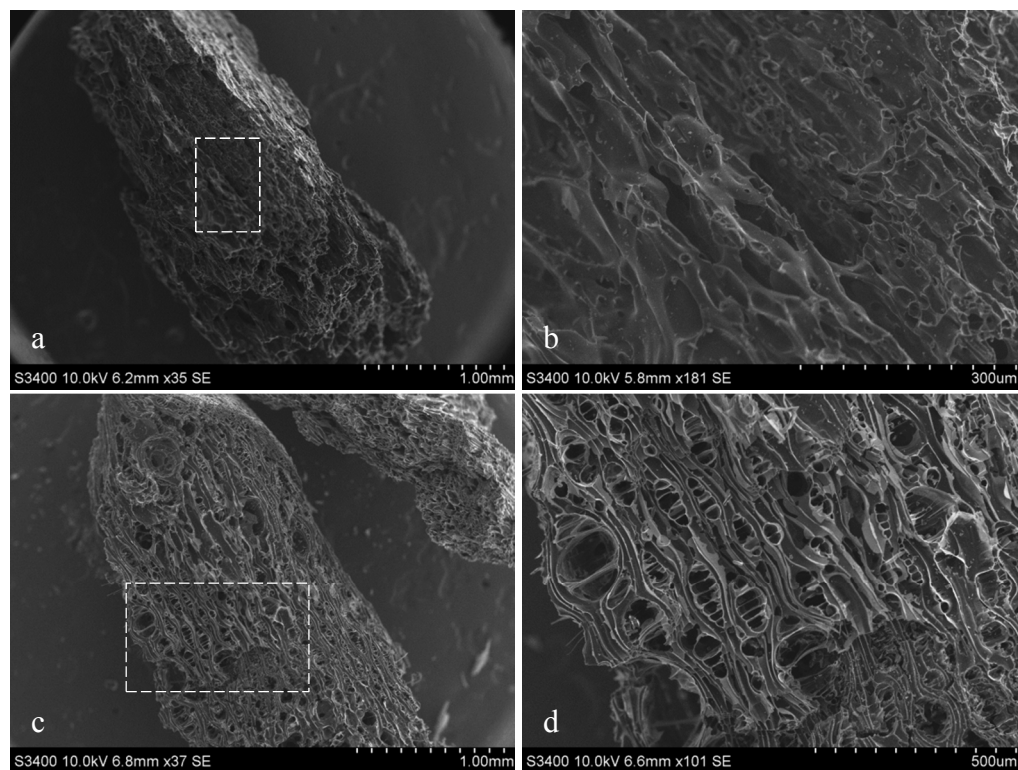
29
30
31
32

Figure 13. SEM micrographs of spruce forest residue charcoal produced in the PTGA in closed crucible at 2.2 MPa

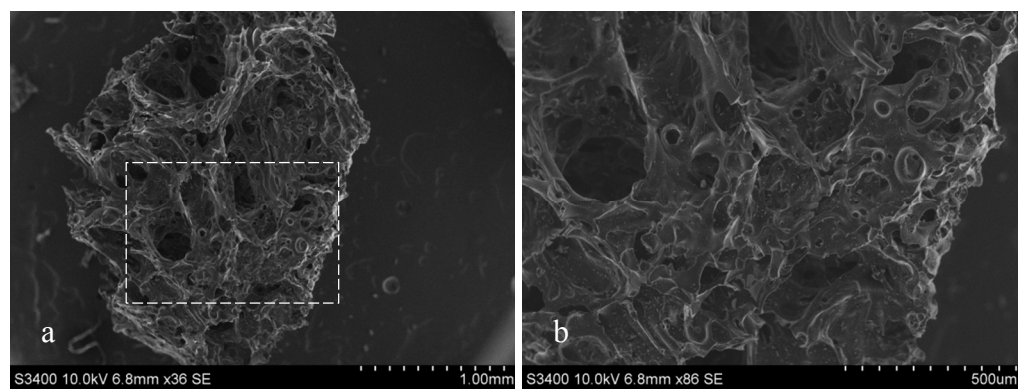


45
46
47
48
49
50
51
52
53
54
55
56
57
58
59
60

Figure 14. SEM micrographs of spruce forest residue charcoal produced in the PTGA in closed crucible at 2.2 MPa



29 **Figure 15.** SEM micrographs of spruce wood charcoal produced in the FC reactor at 0.8 MPa



44 **Figure 16.** SEM micrographs of spruce wood charcoal produced in the FC reactor at 2.2 MPa